CHEMICAL PETROLOGY OF THE PORT COLDWELL ALKALI INTRUSIVE, MARATHON, ONTARIO

CHEMICAL PETROLOGY OF THE PORT COLDWELL ALKALI INTRUSIVE, MARATHON, ONTARIO

By

DAVID J. HERDMAN, B.Sc.

A Thesis

Submitted to the School of Graduate Studies

in Partial Fulfilment of the Requirements

for the Degree

Master of Science

McMaster University

February, 1974

MASTER OF SCIENCE (1974)
(Geology)

McMASTER UNIVERSITY
Hamilton, Ontario

TITLE: Chemical Petrology of the Port Coldwell Alkali Intrusive, Marathon, Ontario

AUTHOR: David J. Herdman, B.Sc.

SUPERVISOR: Professor Brian J. Burley

NUMBER OF PAGES: i-x; 1-88

SCOPE AND CONTENTS:

This study was planned as a combination of detailed field mapping, thin section petrography, whole rock geochemistry and amphibole chemistry of the rocks of the Port Coldwell intrusion.

It was hoped that the results of the detailed field mapping would give a clearer picture of the stratigraphy and structure of the intrusion. It was hoped to define the mineralogy and textures of the various phases of the Port Coldwell intrusion enabling a postulation of possible physical conditions under which crystallization occurred.

Through whole rock chemical analysis it was hoped to correlate the petrochemistry with the stratigraphy, and so to provide a chemical explanation of the differentiation process. Furthermore, it was hoped to classify the gabbros and through differentiation trends provided by the plots of the analyses, to determine whether the gabbro could be a feasible parent of the other phases of the intrusion.

The amphibole found in each phase of the intrusion was to be determined in order to discover elemental trends and to provide corroborating evidence of a differentiation sequence suggested by other sources.

TABLE OF CONTENTS

LIST OF TABLES

LIST OF FIGURES

ABSTRACT

The Port Coldwell intrusion is an alkaline intrusion of the miaskitic type located near the reported triple junction of three gravity-magnetic highs. The complex probably is the result of intrusion of an alkali gabbro and its differentiation products. The classical differentiation sequence was from a parental alkali gabbro, which separated ilmenomagnetite and Fe-Mg pyroxene giving rise to a syenitic magma that differentiated to produce nepheline syenites by a trend towards undersaturation. The same syenitic magma may have assimilated some silica-rich country rocks causing the magma also to have an oversaturation trend producing quartz syenites and granites.

The lamprophyre dykes, stratigraphically the youngest, may have been derived from a primitive magma late in the differentiation sequence. The field occurrence of carbonate ocelli in the lamprophyre dykes of the Port Coldwell intrusion can best be explained using a liquid immiscibility model.

The fine-grained gabbros located north of Neys Provincial Park, which were previously interpreted as a metavolcanic roof pendant, is re-interpreted as a phase of the Port Coldwell intrusive, related to the coarser-grained alkali gabbro. This fine-grained gabbro may have differentiated higher in the crust as a later differentiate of the alkali gabbro after the separation of ilmenomagnetite. The greater volume of syenitic rocks relative

to the parental gabbro may be due to the previous interpretation of substantial volumes of fine-grained gabbros as metavolcanic roof pendants.

Locally high oxygen fugacities existed in the alkali gabbros. A relatively high fluorine fugacity existed in the syenites while a high CO_2 fugacity prevailed in the nepheline syenites and lamprophyre dykes. Water pressures of approximately 4000 kg/cm^2 prevailed in the granitic phase of the Port Coldwell intrusive.

The amphiboles of the Port Coldwell intrusion show a definite increase in Fe with increasing Niggli mg values. The increase in values of Niggli mg in the amphiboles from those in the granite to those in the quartz syenite to nepheline syenite to syenites and lamprophyre dykes, correlates with the decreasing basicity of the host rocks. With decreasing values of Niggli mg, there is a decrease in Mg, Al and Ca in the amphiboles. Na and Si values are relatively constant except for a sharp increase within the amphiboles of the granitic phase.

The amphibole within the syenitic phase is a kaersutite that sometimes possesses characteristics intermediate with barkevekite. The amphiboles in the nepheline syenite and quartz syenite phases are barkevekites, while those in the granites are arfvedsonites. These amphiboles, which represent a solid solution series, suggest a differentiation sequence of cogenetic host rocks.

ACKNOWLEDGEMENTS

Thanks go to Dr. B.J. Burley, my thesis advisor who suggested the Port Coldwell intrusive as a study area. I would also like to thank Dr. K.L. Currie (E.M.R.), Dr. D.H. Watkinson (Carleton University) and Dr. H.D. Grundy (McMaster University) who provided some valuable suggestions. Paul Mainwaring did the amphibole analyses on the electron microprobe at Carleton University in Ottawa. Mr. John Muysson was instructive in the wet chemical analyses and some of the analyses were done by him. I also thank K. Shewbridge, who was my field assistant during the summer of 1972. Financial support for the project came through the National Research Council of Canada and McMaster University

CHAPTER 1

FIELD RELATIONS

Introduction

The Port Coldwell intrusive is located on the north shore of Lake Superior (see Figure 1) within the eugeosynclinal portion of an Archean volcanic-sedimentary belt (Puskas, 1970). These volcanics and sediments of the Superior province have been tightly folded in a north 70° east trend and also folded along another axis in a more northerly trend (Puskas, 1970). Along the western contact of the intrusion, well-bedded proximal turbidites with a high proportion of sandy beds predominate. Emplacement of the intrusion was accomplished by doming and stoping creating a thermal aureole within the pyroxene-hornfels facies (Puskas, 1970). The contacts between country rock and gabbro are sharp and often are intruded by pegmatites while contacts between country rock and syenite are often brecciated and some assimilation commonly has taken place to produce a hybrid syenite.

The Port Coldwell complex is a roughly circular intrusion, with an outer rim of gabbro enclosing syenites, nepheline syenites, and granitic rocks (see Figure 2). The relative stratigraphic sequence (increasing age downwards) of intrusions is as follows (Puskas, 1967):

Precambrian:

Port Coldwell Igneous Complex

Little Pic River Granite
(I.C.)
Lamprophyre Dykes
(I.C.)
Nepheline Syenite
(I.C.)
Quartz Syenite (Nordmarkite)
(G.C.)
Syenodiorite
(G.C.)
Syenite (Laurvikite)
(Conformable, partly G.C.)
Gabbro
(I.C.)

Country Rocks and Roof Pendants:

Archean mafic and felsic metavolcanics
and metasediments

I.C. - intrusive contact

G.C. - gradational contact

Structural features of the intrusion, such as igneous layering and faults have never been mapped. Fine- to medium-grained xenoliths of mafic rock occur randomly through the complex, and although mapped as country rocks by previous workers, may be

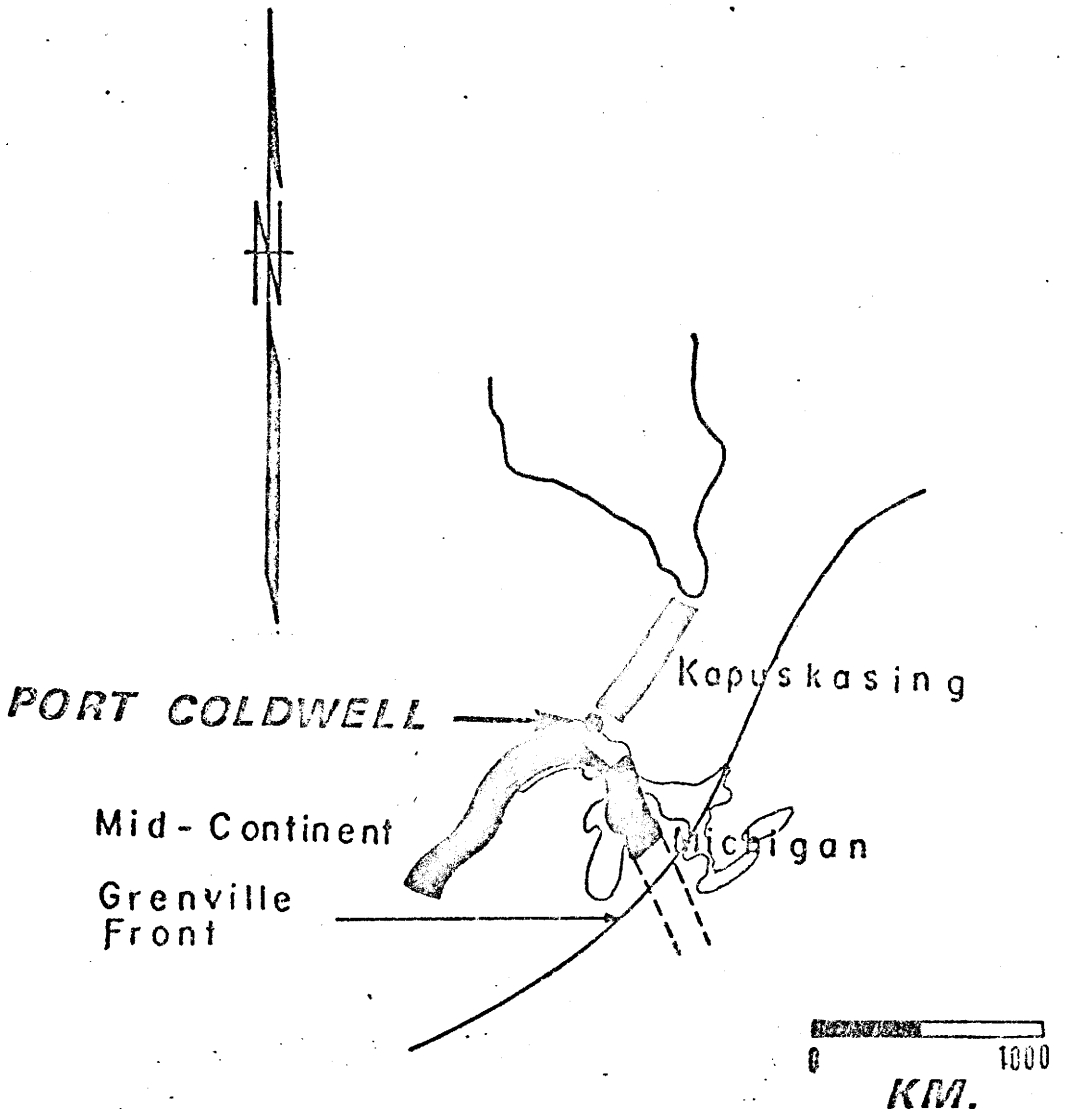

Fig. 1 Location of Intrusive relative to Triple Junction of Gravity-Magnetic Highs (Kevin Burke, personal comm., 1973). (see Basement map of the United States, Bayley and Muelberger, 1968).

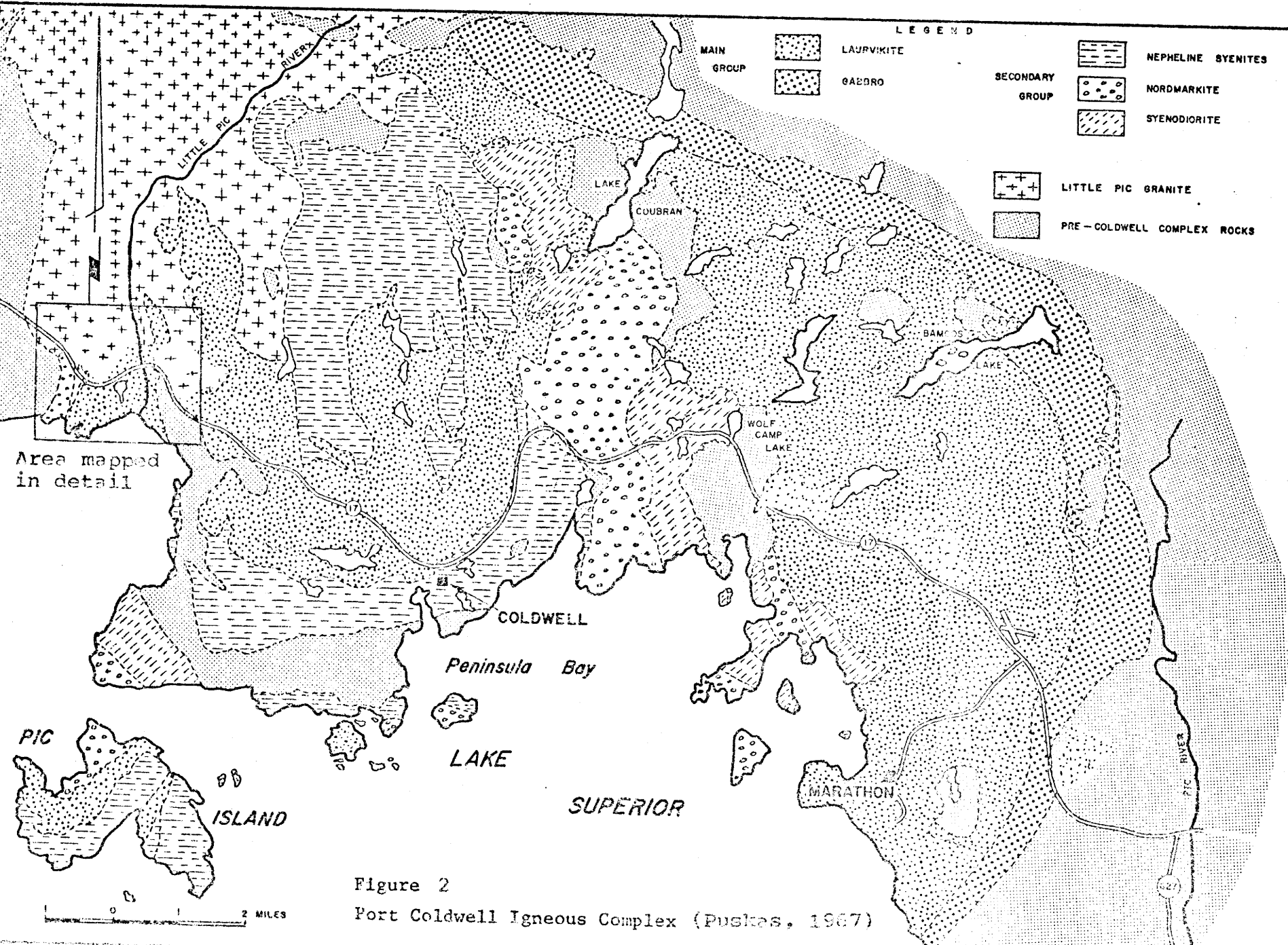

Figure 2

Port Coldwell Igneous Complex (Puskas, 1967)

genetically related to the outer rim gabbros (see Figure 2). The relationship of the granite to other phases is uncertain.

Detailed mapping was carried out using as a guide the large-scale reconnaissance map prepared by F.P. Puskas for the Ontario Department of Mines (see Figure 2). In the summer of 1972, over one month was spent doing detailed geological mapping with a field assistant. This area for detailed mapping was chosen since all rock types were present, access was good and the rocks were well-exposed. The base maps and air photos used were obtained from the Ontario Department of Natural Resources. An aeromagnetic map was used to correlate structural features.

Age and Location Relative to Major Tectonism

Paleomagnetism and geochronology suggest only one period of emplacement, 1050 million years ago (Watkinson, Mainwaring and Lum, 1972). Potassium argon ages of 1005 million years (±1 m.y.) have been determined from biotites from the nepheline syenites of the western lobe of the Port Coldwell intrusion (Currie, pers. comm., 1972). These ages are similar to those of the Keeweenawan intrusives located along the Mid Continent gravity magnetic high (1000 m.y. ±1 m.y.) and to the alkaline intrusives located along the Kapuskasing gravity magnetic high. No intrusives are known to occur along the Michigan gravity magnetic high. The Port

Coldwell intrusive is located near the triple junction of these three gravity magnetic highs (see Figure 1).

Hans Cloos, by experimenting with balloons under clay, has shown that a triple point occurs directly under the swelling balloon. The triple point near which the Port Coldwell intrusive occurs may be the previous site of an upwelling mantle plume (K. Burke, pers. comm., 1973).

Alkali Gabbro

Although the features to be described apply specifically to the area mapped in detail (see Figure 3), they appear, on the basis of cursory examination, to apply generally to the intrusion as a whole.

The alkali group is rhythmically layered with alternating mafic (pyroxene, ilmenomagnetite and biotite) and plagioclase-rich bands (see Plate 1). The dips of the layers in this coarse-grained rock are towards the centre of the intrusion and vary between 5° near the contact with the country rocks, and 70° in other parts (see Figure 3). The strike of this layering is parallel to the strike of the contact between the gabbro and country rocks. Along the contact of the alkali gabbro and laurvikite, rhythmic layering is thin (1-2 mm) and the rock is fine-grained. This fine-grained gabbro is sometimes brecciated by the laurvikite (see Plate 27).

WEST CONTACT OF THE PORT COLDWELL ALKALI INTRUSIVE

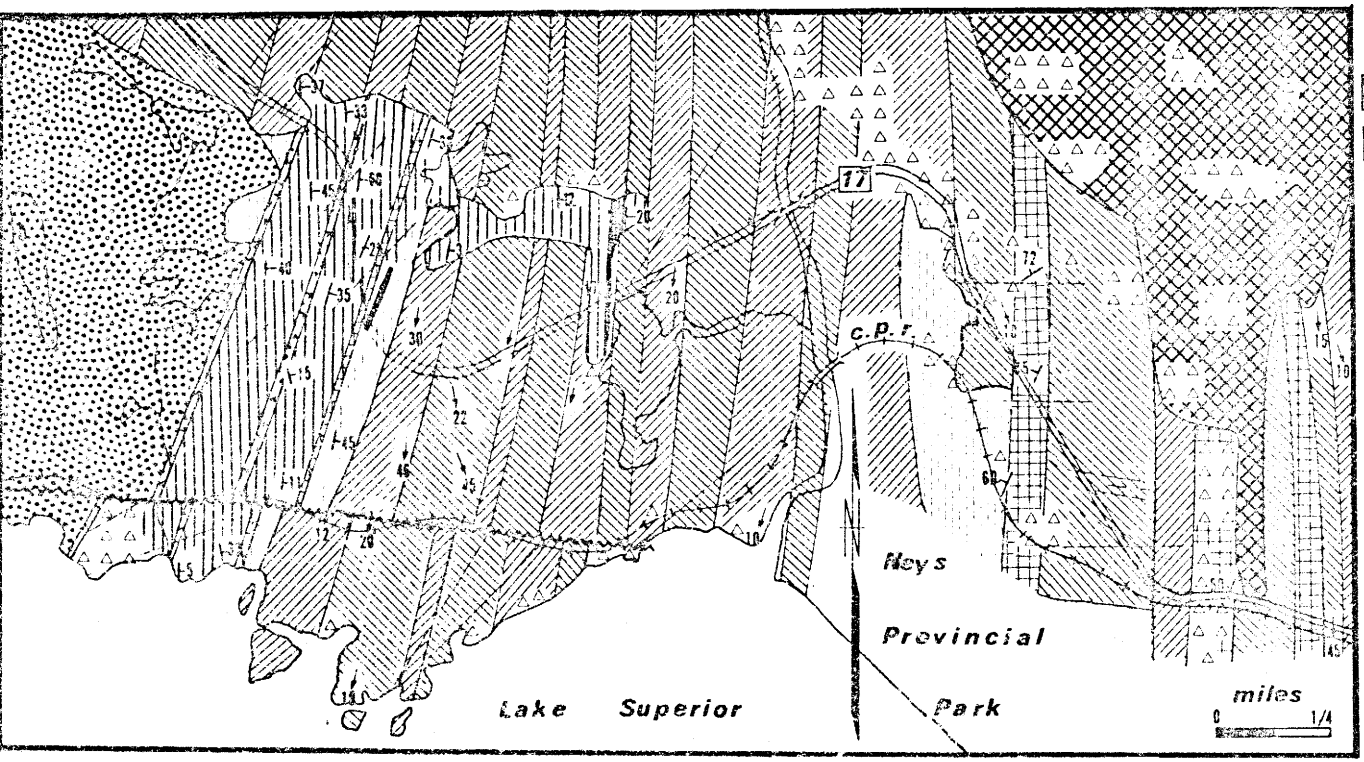

LEGEND

Precambrian

- Pink Granite
- Camptonite Dykes
- Nepheline Syenite

Syenites:

- Pegmatite Sills
- Red Laurvikite
- Black Laurvikite

Alkali Gabbro:

- Layered & Coarse-Grained
- Weakly Layered & Fine-Grained
- Magnetite Segregation
- Brecciated Gabbro

Country Rock:

- Bedded Metagreywacke

Feldspar Lineation

Igneous Layering

Figure 3

Ilmenomagnetite-rich layers occur as lensoid conformable segregations within the coarse-grained layered gabbros (see Figure 3). Sulfides occur along the contact of the coarse-grained layered gabbro and country rock. Chalcopyrite, pyrrhotite and malachite comprise up to 5% of the gabbro. This location at the contact may suggest the separation of a sulfide-immiscible liquid to the periphery of the original magma chamber. The gabbro contacts are offset by a fault (see Figure 3). The fault shows as an air photo lineation and an aeromagnetic map correlates favourably with the existence of a fault. Epidote-coated slickensides plunging steeply south, are common along the length of the fault.

The coarse-grained layered gabbro appears to form a partial ring around the intrusion (see Figure 2). In the area mapped in detail, the ring is cut on the north by the laurvikites and disappears under the waters of Lake Superior to the south.

Neys Park Fine-Grained Gabbro

This supposed xenolith, located north of Neys Provincial Park, is enclosed by laurvikites (see Figure 3). The rock is fine- to medium-grained and closely resembles the fine-grained gabbro occurring in the outer margin of the alkali gabbro where it contacts the laurvikites. The "xenolith" may be brecciated

by the laurvikite. Layering was measured and its strike is the same as the strike of layering in the coarse-grained alkali gabbro, but dips west rather than east, as in the outer rim.

The "xenolith" was previously mapped as country rock, yet bears a striking resemblance to the layered gabbros. The meta-volcanics outside the intrusion are tightly folded, but there is no evidence of folding of the layering in the rocks within the "xenolith".

To the north and north-east of the Neys Park, within the granites and laurvikites, fine- to medium-grained blocks of gabbro may comprise up to 40% of the host rock. This breccia is probably related to the Neys Park "xenolith". Some of the blocks are coarse-grained and have strong rhythmic layering similar to that which occurs in the gabbro recognized as being part of the Port Coldwell intrusive. These striking similarities suggest that the Neys Park "xenolith" and the inclusions within the rocks surrounding the "xenolith" are genetically related to the gabbros of Port Coldwell and are not in fact blocks of country rock as previously interpreted.

Syenites (laurvikites)

There are two types of syenites - pegmatite sills which cut the alkali gabbro and rhythmically layered laurvikite (see

Figure 3). Laurvikites are syenites in which the feldspar is a perthite that usually constitutes more than 80% of the rock.

The pegmatites are low in mafic content and extremely coarse-grained (see Plate 1, Table 1). These pegmatites form sills that are very irregular in width and may pinch out at places. Many smaller ones have not been mapped. Megascopic colour zoning is common in the alkali feldspars of the pegmatitic variety (see Plate 5) and it is manifest as alternating red and black zones. The same phenomena has been recognized in Norwegian rocks. Using the electron microscope, it was determined that the red colour was due to exsolution of hematite oriented as a fibrous felt in planes parallel to 010 (Rosenquist, 1965). The black varieties lack this exsolution.

Large-scale red and black rhythmic layering occurs in the laurvikites. It is probably due to alternating colouration in the alkali feldspars which compose up to 90% of the rock (see Table 1). Varying oxygen fugacity may cause this alternation by its affect on the feldspars. The black layers are not always black, but may be grey-green (see Plates 2,3). Contacts between layers are gradational and difficult to photograph. Lineations trending parallel to the large-scale rhythmic layering are defined by parallel alignment of perthite crystals (see Plates 2,3).

Nepheline Syenites

Two varieties are present - a leucocratic, pegmatitic variety occurring as a sill in the alkali gabbro (see Figure 3), and a melanocratic, medium-grained variety also occurring in sills (see Plates 6,7). Both varieties brecciate the gabbro.

Nepheline, on weathered surface, is easily identified since it alters readily to an orange-brown hydronephelite (see Plate 7). In melanocratic varieties, nepheline-rich clots appear commonly (see Plate 7). They may be nucleation centres. Rhythmic layering, although not always present, is defined by amphibole-rich layers and feldspar-rich ones (see Plate 6). Rhythmic layering in the nepheline syenites, when present, has the same strike as the layering in the laurvikites and alkali gabbros.

Camptonite Dykes

These fine-grained dykes probably follow the dominant joint directions within the intrusion (see Figure 3). The dykes are often columnar jointed and contacts with adjacent rocks are commonly sharp (see Plate 9). Carbonate segregations may occur on the sides of the dykes and off-shoots of these segregations may emenate as veins from the side of the dykes (see Plate 10).

Plagioclase phenocrysts with their long dimension parallel

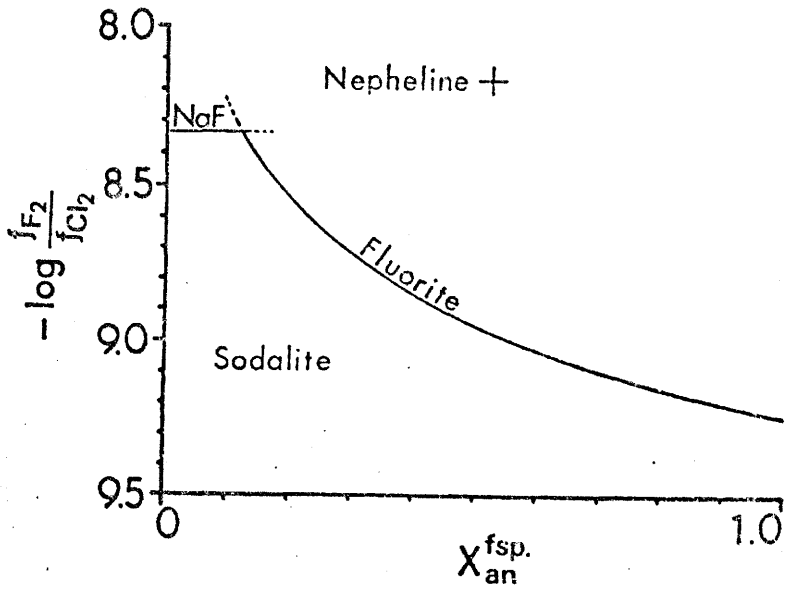

Figure 4. Stability field of sodalite as limited by high ratios of fluorine to chlorine at 1200°K. If a feldspar containing more than 10 mole percent anorthite coexists with sodalite, fluorite plus nepheline will take the place of sodalite with the ratio of fluorine to chlorine falling with increasing anorthite (Stormer and Carmichael, 1971).

to the strike of the dyke may define a trachytic texture. Ellipsoidal carbonate ocelli often define a trend with their long direction parallel to the strike of the dyke (see Plate 9). Carbonate-rich layers abundant in ocelli commonly alternate with layers poor in ocelli defining a layering which is also parallel to the strike of the dyke (see Plate 8). On the weathered surface, the carbonate is often weathered out leaving holes where the ocelli used to occur (see Plate 8).

Origin of Carbonate Ocelli

The carbonate ocelli present in lamprophyre dykes of other studies have been previously interpreted as amygdules, nucleation centres and as immiscible liquid droplets. Melting experiments done on an olivine kaersutite lamprophyre dyke, bearing carbonate ocelli, showed that the rock melted to a homogeneous silicate liquid and an immiscible CO_2-rich liquid phase (Ferguson and Currie, 1970). This suggests that the carbonate ocelli are immiscible liquid droplets frozen into the silicate phase. It would be expected that complete segregation of the immiscible carbonate liquid fraction would occur with slower cooling.

The liquid immiscibility model for explaining the carbonate ocelli may not contradict the amygdule idea, but may explain the formation of amygdules. Amygdules may be liquid

droplets themselves. Escape of the gaseous phase from the amygdule may lead to the formation of a vesicle. Amygdules are usually explained as late-stage fillings of some existing pore space, possibly by groundwater solutions. This theory has the flaw that the pore spaces in igneous rocks are rarely connected to allow any passage of fluids into the vesicle which the carbonate-rich fluid is proposed to fill.

The liquid immiscibility model fits the field observations on the occurrence of carbonate ocelli in the lamprophyre dykes of Port Coldwell. In dykes which have columnar jointing, indicating rapid cooling, the carbonate ocelli are abundant. This may correspond to the separation of a lighter, immiscible fraction into droplets which begin to rise through the denser silicate phase (see Figure 5 and Plate 9). In dykes without columnar jointing, a carbonate-rich fraction may occur at the margin of the dyke (see Plate 10). If the dyke intrudes vertically, carbonate segregations may occur on both sides of the dyke. In dykes having these segregations, the main part of the dyke may have fewer carbonate ocelli. According to the liquid immiscibility model, this segregation would be explained as a collection of the lighter carbonate phase at the tope of the dyke in response to a density difference with the silicate phase.

Stage 1: At P_1, T_1 immiscible CO_2-rich fluid phase begins to dissociate and rise as droplets through denser silicate liquid.

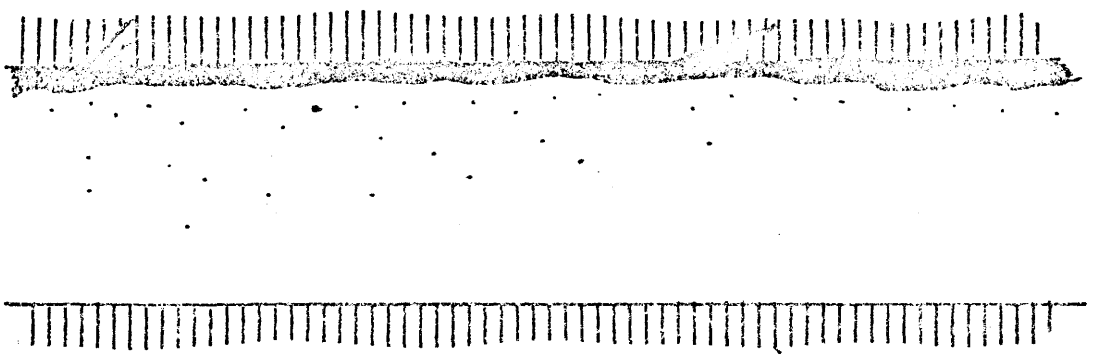

Stage 2: Complete segregation and veining of host rock

0 2

Metres

FIG 5 Stages of Ocelli formation in Camptonite Dykes

Quartz Syenite-Granite

The quartz syenite, described locally as nordmarkite, because the feldspars are perthites, appears to grade imperceptively into granite with increasing quartz content. This leucocratic, coarse-grained unit is very similar in appearance to the red laurvikites of the intrusion. The quartz is extremely difficult to see in the fresh surface. The unit weathers to a low relief and shows up well on the air photos as a somewhat low area relative to the surroundings, with a denser tree cover. Contacts with other units are often obscured by vegetation.

This distinct rock unit is not layered and unlike the laurvikites, has no lineations. A considerable volume of gabbro is present (up to 40%) as inclusions (see Figure 3). Distinct layering, similar to that observed in the alkali gabbro, is present in some of the blocks. This suggests that these inclusions may be an earlier phase of the Port Coldwell intrusion related to the alkali gabbros.

CHAPTER 2

THIN SECTION PETROGRAPHY

Introduction

The amphiboles in the syenite and nepheline syenite phases of the Port Coldwell intrusive have been optically interpreted as barkevekites (Puskas, 1967). Optical identification within the kaersutite-barkevekite series is impossible, since these calcic amphiboles have similar ranges of refractive indices, extinction angles, absorption colours and optic angles (Wilkinson, 1961; Bose, 1963). Birefringence in these amphiboles is almost impossible to determine due to high absorption in thin section. Data on the optical properties of arfvedsonite found in the granites (see Chapter 4, Amphibole Chemistry) is not well-defined (Deer, Howie and Zussman, 1965), but has optical properties similar to kaersutite and barkevekite with whom it may form a continuous solid solution series (Frisch, 1970).

Petrographic Methods

Approximately 100 thin sections from the detailed map area and other parts of the intrusion were studied using a Zeiss polarizing microscope. Modal analyses were made with the use of

a Swift automatic point counter. Mineral proportions of the first 800 points were converted to percentages.

Rocks thought to contain nepheline were stained with malachite green to impart a bright green to the nepheline which otherwise was difficult to distinguish from the alkali feldspars. These alkali feldspars were often stained yellow by Na cobaltinitrite stain which also aided the distinction. Where the alteration of either mineral was extensive, the stains were unsuccessful. Alizarine red stain was used on the carbonate ocelli of the lamprophyre dykes in order to determine whether the carbonate was calcite or dolomite.

Refractive indices of a scapolite and a biotite (Nz only) were determined using Schillabers refractive index oils. Separation of minerals was accomplished by dry sieving the rock powder to 100-150 mesh, wet sieving, then separation by a Franz magnetic separator.

Numerous photomicrographs were taken using an Asahi Pentax with a microscope adaptor on a Zeiss polarizing microscope. Kodak Photomicrography colour film (Estar base) SO-456, 35 mm was used to obtain superior fine-grained results. The film speed is ASA 20 when used with a 90A blue filter to convert the tungsten source to a daylight source.

Alkali Gabbro

Fresh plagioclase (labradorite) is the main constituent of the alkali gabbro (see Table 1). Parallel alignment of labradorite laths often define a lineation (see Plate 11). Rhythmic layering is defined by plagioclase-rich layers alternating with mafic layers. The plagioclase may have strong normal zoning from labradorite to andesine.

Augite is the next most abundant mineral (see Table 1). Along with ilmenomagnetite, amphibole and biotite, it constitutes the mafic layers of the alkali gabbro. Hourglass zoning and twinning in the augites is common (see Plates 13,14). Schiller inclusions of a late exsolved, Ti-rich mineral possibly rutile, suggests a high Ti content (see Plate 15). These pyroxenes are usually a non-pleochroic grey-green, but in ilmenomagnetite-rich layers are often anomalous pink suggesting a high Ti content. A brown to green pleochroic amphibole sometimes occurs as a uralitic rim on pyroxene. The pleochroic scheme is variable with X - pale brown, Y - violet-grey, Z - dark brown with 2V = 70°+.

The pleochroic schemes of biotite vary, e.g. X - light yellow or light brown, Y - deep brown or red-brown and Z - dark brown or deep red-brown. The biotites are spatially related to ilmenomagnetite and augite around which they may form a rim. Determination of the refractive index (Z = 1.65) indicated a 27% $FeO+2(Fe_2O_3+TiO_2)$ content (Deer, Howie and Zussman, 1965).

The reddish-brown colour of the biotites indicates a high titanium content (Deer, Howie and Zussman, 1965). Biotite is more abundant in the gabbros of the eastern rim of the intrusion. This suggests that a higher water pressure may have prevailed in the eastern rim (see Figure 3).

Olivine (Fo 43-67) (Watkinson, Hainwaring and Lum, 1972) occurs in minor amounts in the coarse-grained gabbro. One sulfide-rich layer in the detailed map area seemed to have a higher olivine content than most of the rocks that were examined. Modal analysis of this layer of the alkali gabbro is as follows: plagioclase (labradorite) 70%; olivine 13%; opaques (chalcopyrite, pyrrhotite) 14%; apatite 3%; biotite 2%; augite 1%.

Fine-scale (1-3 mm) layering in the gabbro at the alkali gabbro contact with the laurvikites is similar in mineralogy to that of the coarser-grained variety, although intercumulus phases form a lower volume in the finer-grained phase. In this contact phase, two generations of pyroxene may be present creating a porphyritic texture. Larger, zoned augites may sit in a matrix of smaller plagioclase and pyroxene crystals. This contact phase commonly has an ophitic texture (see Plate 28). Its position along a contact and its similarity to the coarser-grained gabbro suggest that it may be a chilled phase of the alkali gabbro.

Neys Park Fine-Grained Gabbro

These rocks, previously interpreted as metavolcanics, are ophitic textured with fine-scale layering (1-3 mm) parallel to the strike of other layering in the area. These rocks are identical texturally and mineralogically to the contact phase of the alkali gabbro (compare Plates 27 to 29). This suggests that the rocks are a fine-grained gabbro of the Port Coldwell intrusive occurring as a xenolith in a later phase of the intrusion.

Syenites (Laurvikites)

These laurvikites are composed mainly of perthitic feldspars which form a strong lineation (see Plates 2,3). The strongly coloured amphiboles have birefringences ranging from 0.02 to 0.03 and variable pleochroic schemes, e.g. X - muddy-brown or straw-yellow; Y - dark green to red-brown; Z - olive or muddy green, and a high optic angle. These amphiboles may form uralitic rims on pyroxene (see Plate 17). The pale grey-green, non-pleochroic, often zoned pyroxene is a hedenbergite with 2-3% Eu (P. Mainwaring, pers.comm., 1973).

Hybridized laurvikite at the country rock contact of the western margin of the Port Coldwell intrusive (see Figure 3) exhibits some evidence of shearing and assimilation. The feldspars

Table 1. Modal average for common rock types representing ≤25 thin sections for each phase

	Alkali Gabbro		Syenite		Nepheline Syenite		Quartz syenite granite		Camptonite dykes	
	Average Mode	Range	Average Mode	Range	Average Mode	Range	Average Mode	Range	Average Mode	Range
Perthite			83	63-98	78	60-90	78	38-90		
Plagioclase	50	5-85	tr		tr				75	50-95
Pyroxene	26	5-70	3	0-15	1	0-10			4	1-10
Amphibole	10	0-70	15	0-33	7	1-20	7	1-15	10	1-50
Biotite	4	0-12	1	0-8	tr				3	1-8
Quartz			tr				13	2-48	tr	
Nepheline			tr		13	2-37				
Olivine	1	0-12							tr	
Ilmenomagnetite	3	0-15	tr		tr		tr		tr	
Apatite	tr		tr		tr				tr	
Fluorite			tr		tr					
Calcite			tr		tr		tr		4	1-10
Zircon			tr							
Reibeckite	tr									
Scapolite									tr	

all have crenulated margins and there appears to be two generations of feldspars, a smaller twinned variety and a larger zoned, untwinned type.

Purple fluorite is a common accessory (see Plate 16) of the laurvikite. It has been reported that the colouration in these may be due to the rare earths Eu^{+2} and Gd^{+3} (Bill, Sierro and Lacroix, 1967). The presence of fluorite may indicate conditions under which the rock formed. Nepheline and fluorite are stable, if the rocks have sufficient calcium to form feldspar with greater than 10 mole percent anorthite, and a partial pressure ratio of chlorine relative to fluorine of less than 10^8 (see Figure 4). If these conditions are not met, sodalite may form possibly according to a reaction such as:

$$2 \text{ sodalite} + \text{anorthite} + F_2 = \text{fluorite} + 8 \text{ nepheline} + Cl_2$$

These relationships remain essentially the same over a temperature range 1000°K - 1400°K (Stormer and Carmichael, 1971).

Within the laurvikite phase, calcite, zircon and biotite are also common accessories. The biotite often occurs as a reaction rim around pyroxene.

Nepheline Syenites

The coarse perthite (see Table 1), as in the laurvikites,

forms a lineation (see Plate 18). Nepheline often is altered to hydronephelite, which is a mixture of many minerals notably natrolite, muscovite, various feldspathoids and alumina minerals (Edgar, 1965). This alteration is most common when nepheline percentage is small.

Texturally the nepheline syenites are similar to the laurvikites and appear to grade imperceptibly into a syenitic composition with decreasing nepheline content. The amphiboles, which are the dominant mafic (see Table 1) have variable pleochroic formulae, e.g. X - straw yellow, yellow-green or olive green; Y - brown to black. The amphibole may be twinned (see Plate 19) and may form a uralitic rim on pyroxene. The minor pyroxene, hedenbergite (P. Mainwaring, pers. comm., 1973) often with regular zoning, is the same pale grey-green pyroxene found in the syenites. Biotite is strongly pleochroic, e.g. X - pale yellow; Y - green brown; Z - brown to opaque.

Camptonite Dykes

The plagioclase (labradorite An 68) is often deuterically altered and often defines a trachytic texture (see Plate 25). Calcite occurs mainly in ellipsoidal ocelli whose longest dimension parallels the probable flow direction defined by the plagioclase crystals. Calcite only rarely occurs as an interstitial

mineral. The carbonate was stained using alizarine red in order to determine that no dolomite was present. The presence of calcite in high amounts (see Table 1) may indicate a high CO_2 fugacity.

The carbonate ocelli are mainly composed of calcite, but in one dyke, the ocelli were composed of a mixture of calcite and scapolite (see Plate 24). The scapolite was a mizzonite with $76\pm7\%$ meonite content. A reaction between the calcite and plagioclase may have occurred to produce this calcium-rich scapolite. In some of the ocelli the assemblage may contain all of the three phases of the possible reaction. Scapolite forms in environments rich in volatiles and a high CO_2 fugacity favours the stability of the calcium-rich end member (Haughton, 1967). Mizzonite has been found as a primary mineral in eclogites (Mathias, Siebert and Ringwood, 1970).

Kaersutite (see Amphibole Chemistry, Chapter 4) occurs as an accessory. It has a variable birefringence and a pleochroic scheme as follows: X - pale yellow; Y - pale green; Z - yellow-green. Augite occurs rarely as phenocrysts giving the rock a porphyritic texture.

Quartz phenocrysts occur rarely in subhedral shapes only in dykes that contain no calcite.

Pink Granite - Quartz Syenite

The main constituent of the quartz syenites is perthite (see Table 1) which, unlike the perthites of the syenites (laurvikites) has no preferred orientation (see Plate 22). Zoning within a single feldspar crystal from an initially homogeneous alkali feldspar to an outer perthitic rim (see Plate 20) may reflect rapid change in water pressure within the quartz syenite magma, rather than falling temperature. A rise in water pressure may have caused the partial unmixing of the alkali feldspar solid solution. An excess of water may have caused a complete unmixing of the feldspar solid solution, producing two separate feldspars (see Figure 6). With an increase in quartz content in the granites of Port Coldwell, a two feldspar system appears. Above a modal percentage of 20% quartz, a twinned, slightly altered orthoclase coexists with an interstitial Carlsbad-twinned albite. With quartz modes between 10-20%, perthite is the common feldspar. This phenomenon may possibly be explained as follows (see Figure 6):at water pressures less than 4000 kg/cm^2, complete solid solution exists, but at higher pressure there are unique fields of albite solid solution and orthoclase solid solution and a true eutectic. The existence of the two feldspars at higher quartz modes in the granites may reflect a greater water solubility in the more silica-rich magma with increasing differentiation.

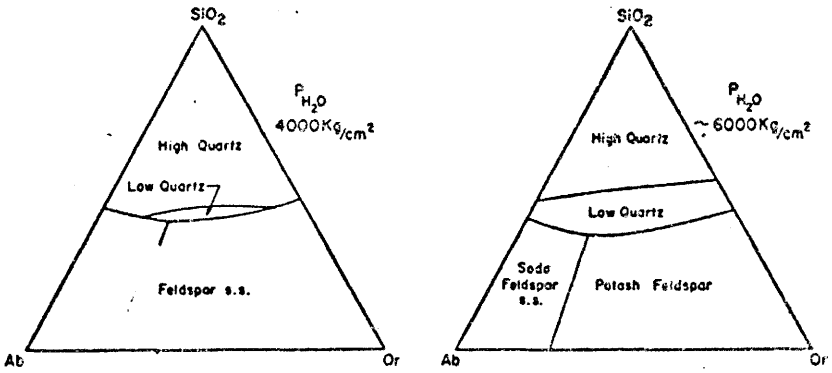

Figure 6. Stability fields at the liquidus in the system $NaAlSi_3O_8$ - $KAlSi_3O_8$ - SiO_2 - H_2O for water pressures approximating crystallization conditions of the granitic phase of the Port Coldwell intrusive (Bowen and Tuttle, 1958)

Amphiboles, constituting a low modal abundance (see Table 1), are the main mafic mineral. In the quartz syenites (nordmarkite of some authors), which grade with increasing quartz content into granites (more than 10% quartz), the amphibole has a pleochroic scheme as follows: X - grey-green; Y - lime-green; Z - dark green, dark brown or opaque. In the granites, the amphiboles are paler green lacking the deep browns, and marked pleochroism common to the amphiboles of the other phase of the Port Coldwell intrusion.

CHAPTER 3

WHOLE ROCK GEOCHEMISTRY

Introduction

Whole rock wet chemical analyses were done on samples selected as type examples from various phases of the intrusion (see Table 2). It was hoped that the relationship of the Neys Park xenolith gabbro (sample 77) to the rest of the layered gabbros would be determined. By the use of variation diagrams, ternary plots and the calculation of agpaitic indices, certain differentiation trends and cogenetic relationships were expected to be established. Also the layered gabbros and Neys Park xenolith gabbros were to be chemically classified and characterized.

Method of Analysis

The elements Mn, Mg, Ca, Na and K were analyzed using a Perkin-Elmer Model 303 Atomic Absorption Spectrometer, with an acetylene flame. Readings were automatically taken and printed by a DCR-1 (digital counter readout). Samples were read at least six times in succession, using a motor-controlled, rotating sampling table. Each sample was aspirated for 5 seconds followed by a 15 second aspiration of air before the next sample. After

Table 2. Modes of chemically analyzed rocks (800 points for each)

	Gabbro					Syenite				Nepheline syenite			Quartz syenite		
	77	35	28	13A	13B	7150	3B	7A	1A	7142	16E	131	11B	7141	4
Perthite						83	63	66	79	63	76	64	74	82	77
Nepheline						2		tr		37	7	17			
Quartz							tr						9	7	9
Plagioclase	45	76	17	52	52			tr			tr				
Olivine	tr	8			tr										
Clinopyroxene	30	5	70	23	30			12	1					4	
Amphibole	13	1		tr	tr	14	33	11	16	tr	12	20	15	6	8
Biotite	9	tr	tr	12	11		tr	8		2			1		
Magnetite	3	9	15	11	6	tr	tr	3	3	tr	2	tr	tr	tr	4
Fluorite							2			tr	1			tr	
Calcite						tr	tr				2				tr
Apatite	tr	tr	1	2	tr										
Zircon									tr						
Sphene				tr	tr										tr

Table 3. Whole rock chemical analyses of various phases of the Port Coldwell alkali intrusive

	Gabbro					Syenite				Nepheline Syenite			Quartz syenite		
	77	35	28	13A	13B	7150	3B	7A	1A	7142	16E	131	11B	7141	4
SiO_2	49.51	35.07	43.80	42.42	48.60	60.06	58.41	52.29	58.19	57.67	61.10	54.92	62.18	64.26	61.74
Al_2O_3	14.98	6.32	15.43	15.30	15.33	18.83	13.79	15.08	13.76	21.88	19.37	21.02	16.67	15.42	16.21
Fe_2O_3	2.90	6.34	4.42	7.12	3.91	2.69	2.87	2.53	2.59	2.00	1.31	1.87	2.12	1.64	4.25
FeO	7.69	30.96	10.32	9.81	6.75	2.32	7.60	8.01	8.89	1.74	1.08	2.72	3.40	3.60	1.65
MgO	7.25	5.55	4.54	5.56	5.83	0.68	0.26	3.17	0.31	0.02	0.16	0.74	0.63	0.24	0.20
CaO	11.11	9.26	11.79	10.25	10.61	0.13	2.96	5.48	4.10	0.59	1.34	1.90	1.64	1.77	1.92
Na_2O	2.75	0.84	3.07	3.09	3.46	5.39	5.58	4.81	5.07	9.53	6.40	7.10	5.67	5.85	6.00
K_2O	1.13	0.49	0.60	1.19	1.30	6.43	4.85	3.91	4.76	4.79	6.66	7.06	5.18	5.43	4.77
TiO_2	0.66	5.45	2.77	2.21	1.19	0.36	0.58	1.09	0.79	0.03	0.09	0.36	0.65	0.38	0.86
MnO	0.18	0.88	0.21	0.24	0.22	0.13	0.37	0.23	0.33	0.10	0.08	0.11	0.14	0.15	0.09
H_2O+	0.91	0.45	0.45	1.31	1.07	1.19	1.00	1.16	0.33	1.10	1.14	0.95	0.77	0.32	0.79
H_2O-	0.71	0.06	0.65	0.46	0.51	0.54	0.18	0.19	0.32	0.19	0.46	0.51	0.38	0.36	0.23
CO_2	0.00	0.00	0.00	0.66	0.09	0.05	0.26	0.34	0.07	0.04	0.15	0.02	0.03	0.04	0.67
P_2O_5	0.33	0.67	1.68	2.04	1.12	0.07	0.07	0.71	0.14	0.00	0.02	0.15	0.12	0.05	0.24

Samples 28, 77, 35 analysed by John Muysson; Sample 77 - Neys Park xenolith

consulting previous analyses, high, low and medium standards were chosen and run with each element. The number of cycles that the sampling table made depended on the quality of the numbers that were printed out. The better the readings, the fewer the number of cycles required.

The raw data was then punched onto computer cards. The programme was designed to reject any value that was greater than 5% from the mean. Any such value would then be replaced by the mean. The three drift components, sensitivity, blank and undulatory drift were computed and the readings corrected. The system is designed on the basis of 0.5 g sample weights.

Agpaitic Index

The agpaitic index for alkaline rocks is defined as $Na_2O + K_2O / Al_2O_3$ (as molecular proportions). Rocks with an agpaitic index greater than one are defined as agpaitic (peralkaline) and those with a lower value as miaskitic (subalkaline) (Gerasimovsky, 1956).

The Port Coldwell layered gabbros have values of the agpaitic index ranging from 0.31 - 0.47. The Neys Park fine-grained gabbro lies within this same range. The syenites vary between 0.60 and 0.97 overlapping values of the nepheline syenites (0.70 - 0.95) and quartz syenites. Thus, the rocks of the Port

Coldwell intrusion are miaskitic.

The results of experiments under different oxygen pressure conditions suggest that in initially undersaturated magmas, low oxygen pressure conditions favour a differentiation trend towards miaskitic rocks (Sood and Edgar, 1970). In early stages of crystallization under low oxygen pressure conditions, rocks may be miaskitic, but with increasing differentiation with increasing oxygen pressures, they may become agpaitic (Sood and Edgar, 1970).

Agpaitic rocks often have high proportions of volatiles such as Cl_2, F_2 and H_2O causing them to have higher melting intervals (Sood and Edgar, 1970). The presence of such volatiles may result in the formation of minerals like sodalite. The lower initial alkali, in comparison to alumina in miaskitic rocks of the Port Coldwell, make this less likely to occur and this is, in fact, reflected in the absence of sodalite in the intrusion.

Chemical Classification of Gabbro

Two norms were computed using a programme for CIPW norms. In one it was assumed that all the Fe occurred as ferrous iron, while the other considered the two (ferrous and ferric) valencies separately. The norms were plotted within the system nepheline-forsterite-quartz, on which igneous rock averages for various types of gabbros are commonly plotted (see Figure 7). The Port

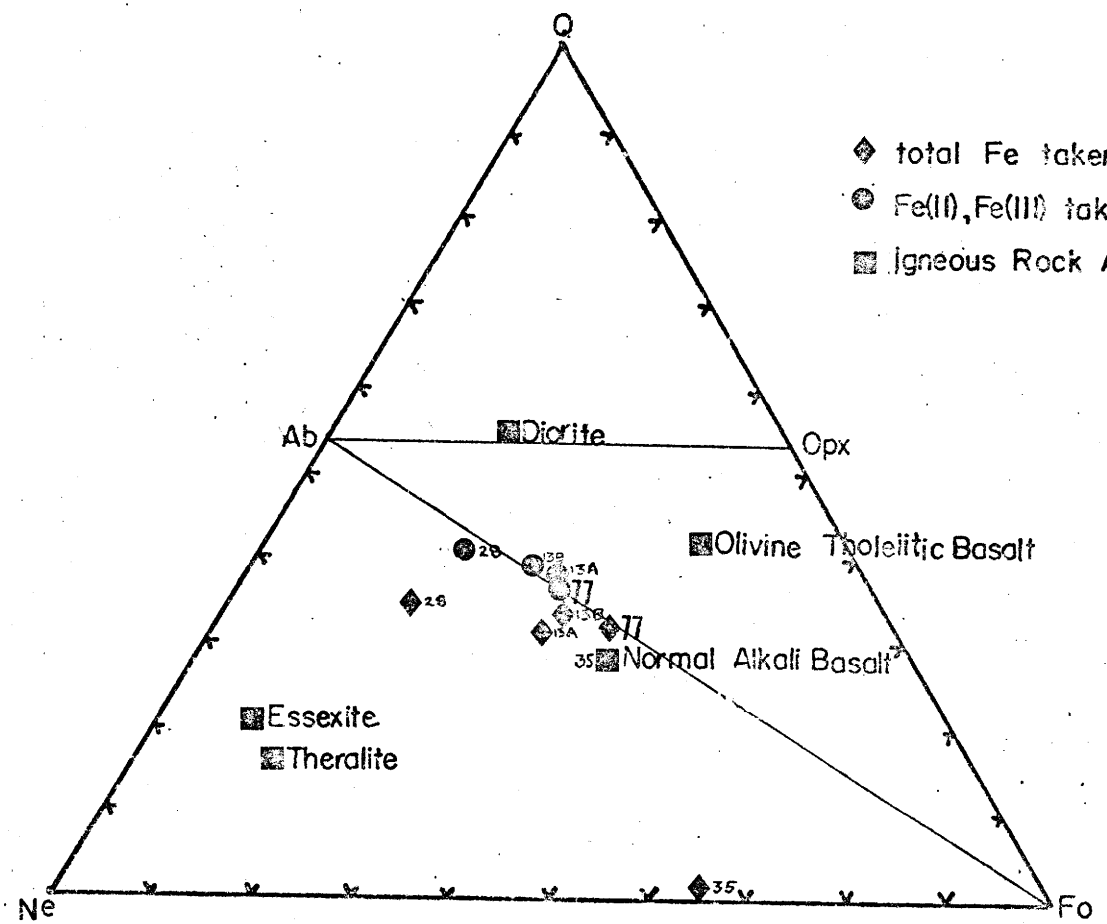

FIG. 1 Base of the Simplified Basalt Tetrahedron
Average igneous rocks from Nockolds(1954)

Coldwell layered, coarse-grained gabbros plot near the normal alkali basalt average and the Neys Park fine-grained gabbro (sample 77) is also close enough to be classified as an alkali gabbro.

The diagram weight percent silica against alkali oxides contains a separating line for subalkaline and alkaline gabbros (see Figure 10). The layered, coarse-grained gabbros plot in the alkaline field, but the Neys Park fine-grained gabbro falls just outside the field of alkaline gabbros. The Neys Park fine-grained gabbro is a xenolith within silica-rich laurvikites. A slight amount of silica enrichment may have occurred, causing a shift towards the subalkaline field.

Ternary Plots

A definite fractionation trend can be seen on the AFM diagram with differentiation successively from alkali gabbro to syenite to quartz syenite (nordmarkite) and nepheline syenite (see Figure 8). The Neys Park gabbro plots clearly on trend, but appears to be less differentiated.

By calculation of norms (see Table 4), one can plot the syenites, quartz syenites and nepheline syenites on a nepheline-kalsilite-silica diagram. The syenites plot on the thermal divide between albite and orthoclase in a region of A, whereas

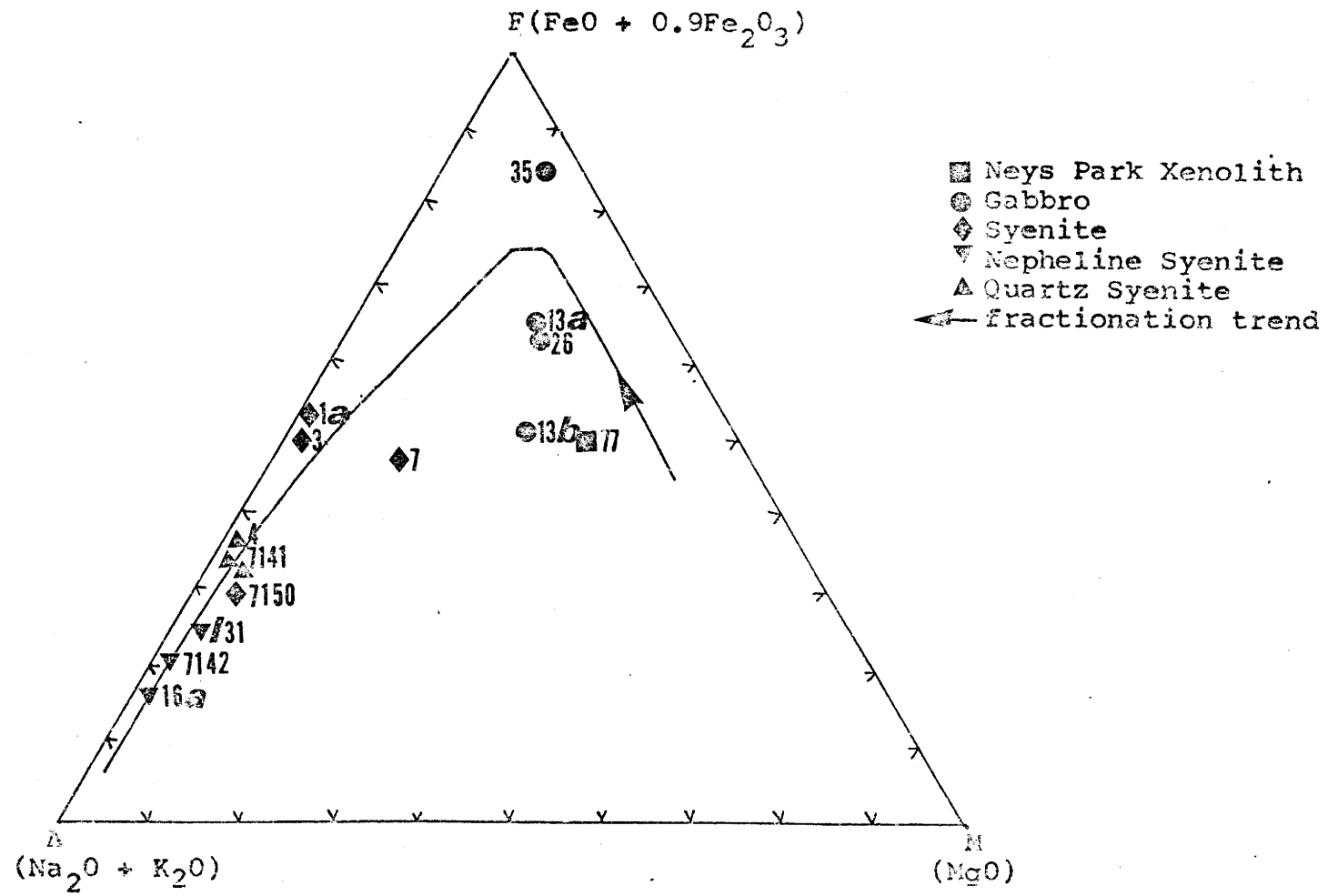

Fig. 8 AFM Diagram showing fractionation trend

Table 4. Norms of chemically analysed rocks (see Table 4A for legend of mineral names)

	77	35	28	13A	13B	7150	3B	7A	1A	7142	16E	131	11B	7141	4
Qtz						2.21							3.91	4.77	6.33
Co						3.33									
Or	6.79	3.16	3.70	7.38	7.83	38.50	29.49	23.60	28.71	27.30	39.10	41.01	30.79	32.15	28.34
Ab	25.10	6.55	27.49	29.11	31.69	49.04	47.99	36.94	46.51	43.20	47.30	22.07	51.22	52.22	54.19
An	25.63	13.12	27.64	19.85	22.92			8.19	0.75	2.58	4.43	4.57	4.78		3.24
Ne		1.00	0.75					4.32		23.70	5.82	24.36			
Di	15.44	7.49	9.97	8.11	12.99		0.68	4.85	1.04		0.32	1.28	0.70	0.89	0.40
He	7.14	18.26	7.46	3.98	5.18		9.68	5.26	13.87		0.55	1.61	1.25	5.69	
Ac							2.86							0.34	
En	3.65			2.25	1.37	1.85	0.28		0.27				1.40	0.22	0.36
Fe	1.69			1.10	0.55	1.49	3.97		3.67				2.50	1.39	
Fo	6.74	9.72	6.05	7.35	6.41		0.09	4.89	0.06	0.04	0.21	1.03			
Fa	3.12	23.68	4.52	3.61	2.56		1.30	5.30	0.81	1.03	0.36	1.30			
Mt	3.08	7.23	4.81	7.81	4.17	2.85	2.02	2.70	2.68	2.02	1.36	1.922	2.23	1.59	2.26
Il	0.94	8.28	4.02	3.23	1.69	0.51	0.83	1.55	1.12	0.04	0.12	0.49	0.91	0.53	1.20
He															1.47
Cc				1.75	0.23	0.13	0.68	0.88	0.18	0.10	0.38	0.05	0.08	0.10	1.70
Ap	0.70	1.53	3.66	4.48	2.39	0.15	0.15	1.52	0.30		0.04	0.31	0.25	0.11	0.51
No	50	67	54	40	42			16	2	6	7	7	9	0	6

Table 4A. Legend of normative mineral names

Qtz	-	Quartz	
Co	-	Corundum	
Or	-	Orthoclase	
Ab	-	Albite	]——Plagioclase
An	-	Anorthite	]
Ne	-	Nepheline	
Di	-	Diopside	]——Augite
He	-	Hedenbergite	]
Ac	-	Acmite	
En	-	Enstatite	]——Orthopyroxene
Fe	-	Ferrosilite	]
Fo	-	Forsterite	]——Olivine
Fa	-	Fayalite	]
Mt	-	Magnetite	
Il	-	Ilmenite	
He	-	Hematite	
Cc	-	Calcite	
Ap	-	Apatite	
No	-	Normative Anorthite Content	

the nepheline syenites and quartz syenites plot outwards from it in different directions in opposing linear trends (see Figure 9). Point A may represent the bulk composition of parental syenite magma from which lead linear trends caused by enrichment or depletion in silica across the thermal divide.

If the syenitic magma represented by point A (see Figure 9) differentiated from the alkali gabbro, then it would tend to differentiate towards a more undersaturated side. In order to get this magma to differentiate towards an oversaturation trend, a small volume of silica must be added in order to cross the thermal divide. Assimilation of a small volume of country rock such as the turbidites which contact the west margin of the intrusive, could initiate the oversaturation trend of the syenitic magma.

Variation Diagrams

The aim of the variation diagrams was to correlate petrochemistry with the observed sequence of field relations to indicate a probable differentiation sequence and to reflect a trend from an initial syenite magma towards differing oversaturated and undersaturated magmas shown clearly in the ternary plot SiO_2-NaAl SiO_4-$KAlSiO_4$. A definite split was expected to appear branching from the laurvikite field into two other phase fields,

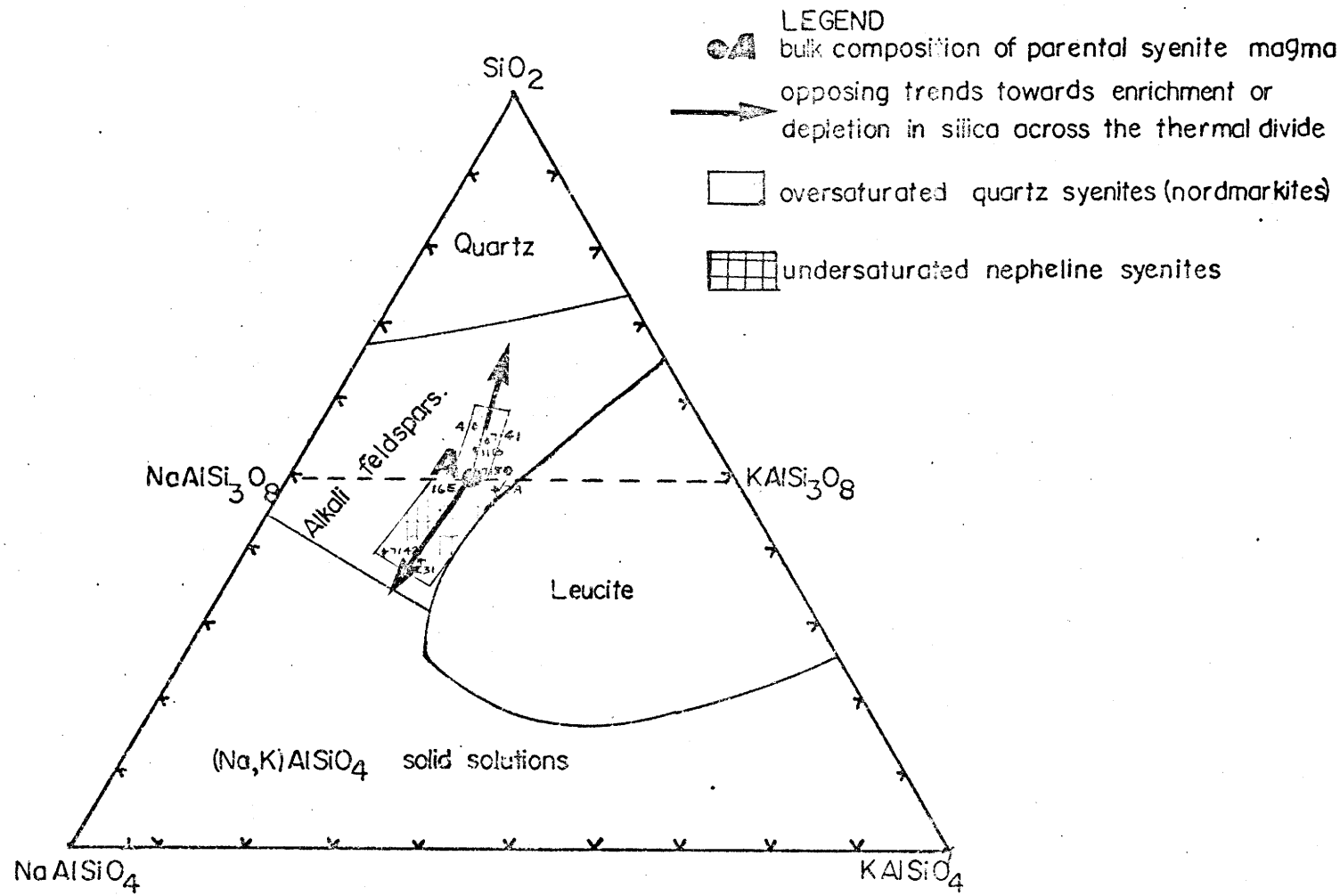

FIG. 9 The System Nepheline–Kalsilite–Silica at atmospheric pressure (J.F Schairer)

possibly with overlap between syenite and quartz syenite or syenite and nepheline syenite. It was hoped that the syenite magma could be shown to be the parent magma of both nepheline syenites and quartz syenites (by contamination).

Differentiation trends were represented as lines which gave a best fit through plotted points. Blocks were drawn around various rock types whose modes were previously determined. The blocks were designed to emphasize the area on the various diagrams occupied by these various rock types. Stippling identified each block and gave a good visual representation.

Simple variation diagrams using weight percent oxides reflect the opposing trend towards undersaturation and oversaturation, as seen by the ternary plot nepheline-kalsilite-silica. In the silica versus alkali oxides diagram, a definite linear trend can be seen starting in the layered alkaline gabbros and moving towards the syenites (see Figure 10). The linear trend splits within the syenites field towards oversaturated quartz syenites and undersaturated nepheline syenites. The quartz syenites plot to the right of the linear trend, defined by the set of points of the other phases. This may point to possible assimilation of country rocks.

Mineralogically, this trend may be explained by enrichment of residual liquid in alkalis by separation of pyroxene and plagioclase in the alkali gabbros. A stronger enrichment manifested by nepheline in the nepheline syenites, is shown relative to the

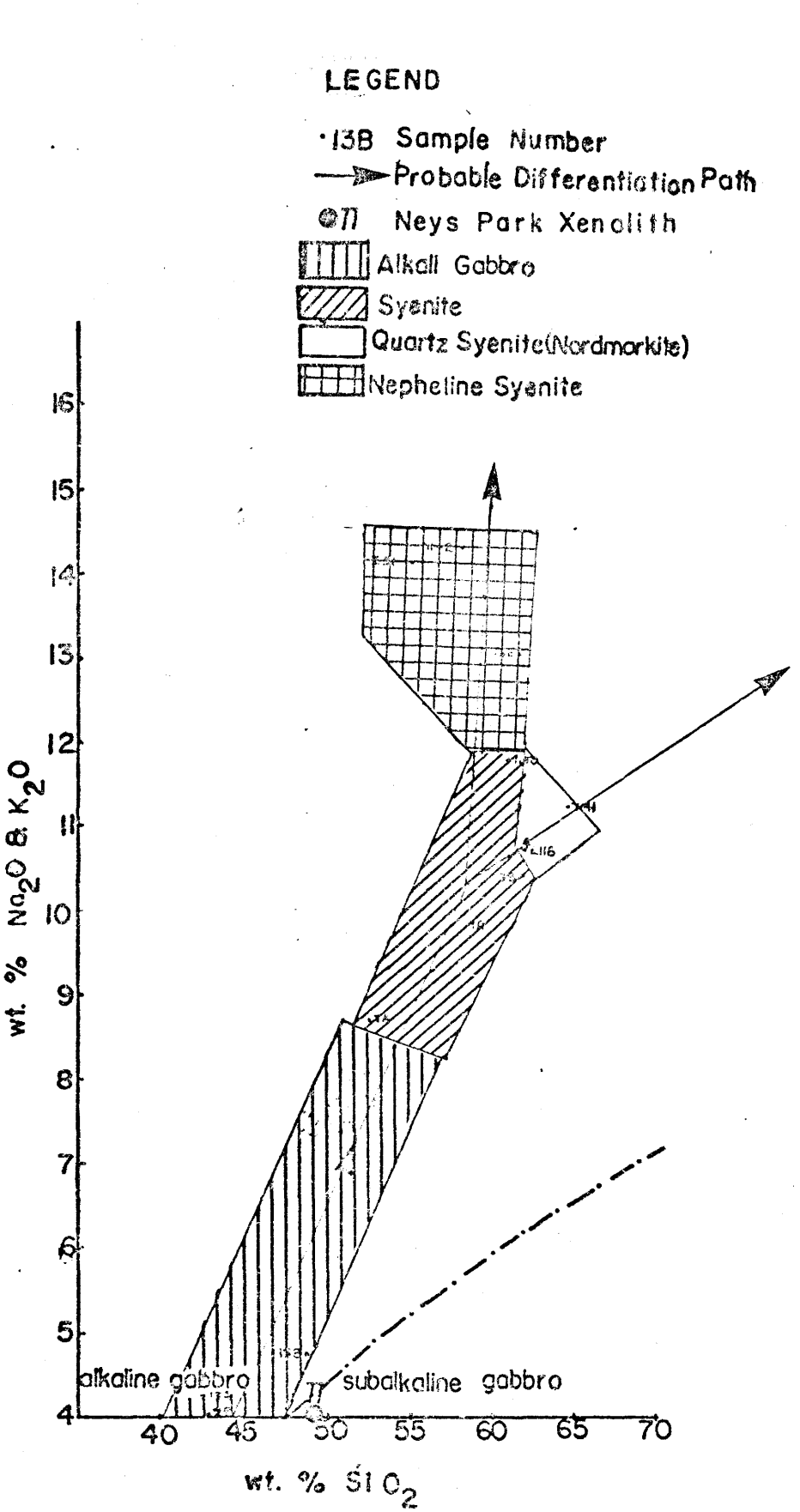

FIG. 10 Weight Percent Silica vs. Alkali Oxides
Gabbro subdivision after Irvine & Baragar(1971)

quartz syenites.

The plot of silica against iron (see Figure 11) shows the same possible differentiation trend with the quartz syenite field lying off to the side of the almost linear trend defined by the alkali gabbro, syenite and nepheline syenite fields. These series of fields suggest a differentiation sequence with the oversaturated quartz syenites as a closely associated phase, perhaps slightly off the linear trend defined by the other phases as a result of assimilation of foreign material.

The decrease in Fe with increase in silica can be explained by an initial loss of Fe due to the separation of large volumes of ilmenomagnetite in the alklai gabbro, then a slower depletion in the other phases due to precipitation of ferromagnesium minerals and some iron oxides.

Weight percent silica against calcium (see Figure 12) shows the same possible differentiation trend as the previous variation diagrams. The Neys Park fine-grained gabbro, previously interpreted as a metavolcanic roof pendant, plots very close to the other gabbros from the Port Coldwell intrusive, and near to the possible differentiation trend suggesting a possible genetic relationship. Separation of large volumes of labradorite in the alkali group would deplete the residual magma in calcium.

In the silica against magnesia diagram (see Figure 13), the same possible differentiation occurs. The alkali gabbros occupy a large, separate diffuse field while most of the other

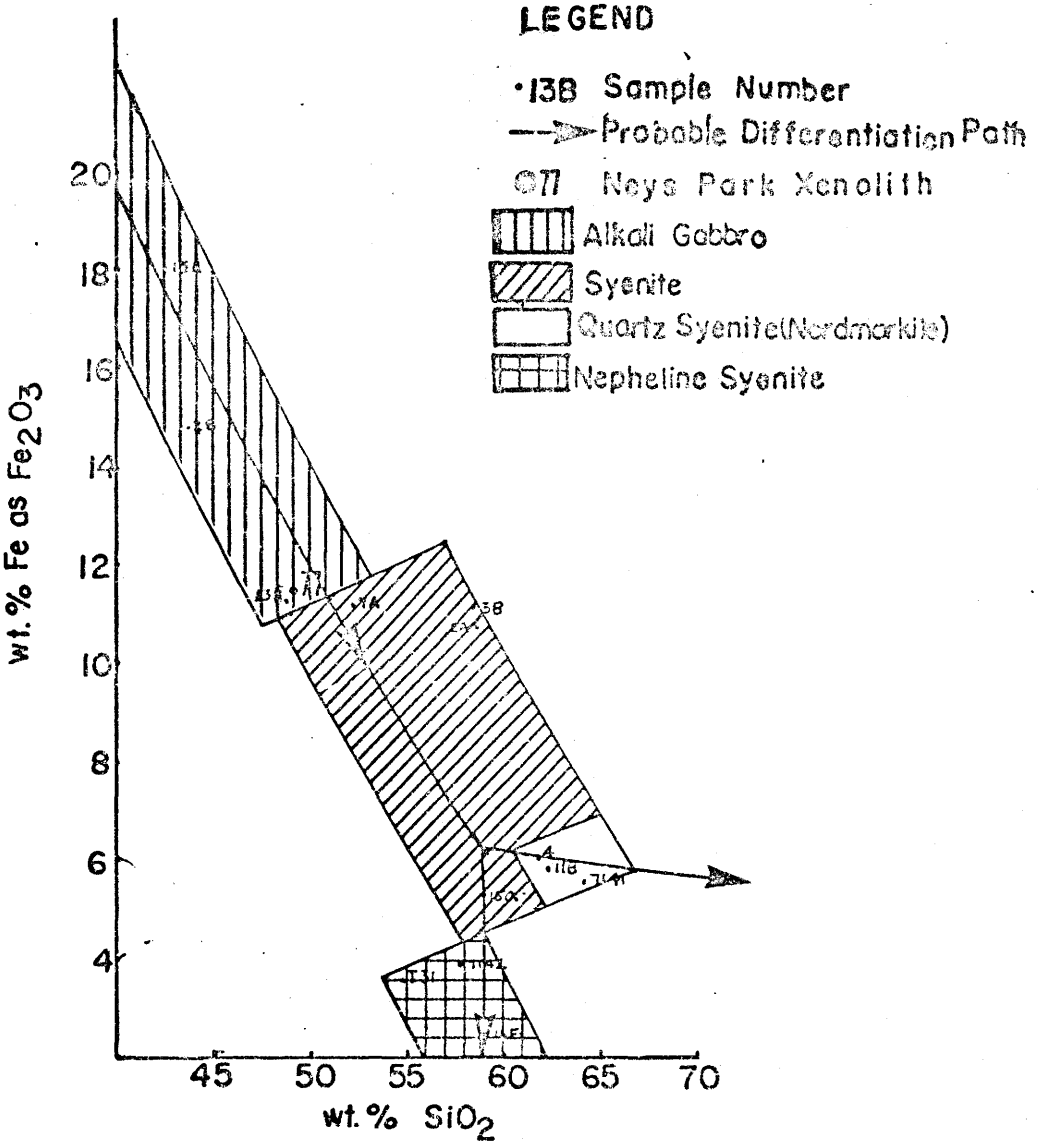

FIG. 11 Weight Percent Silica vs. Total Iron

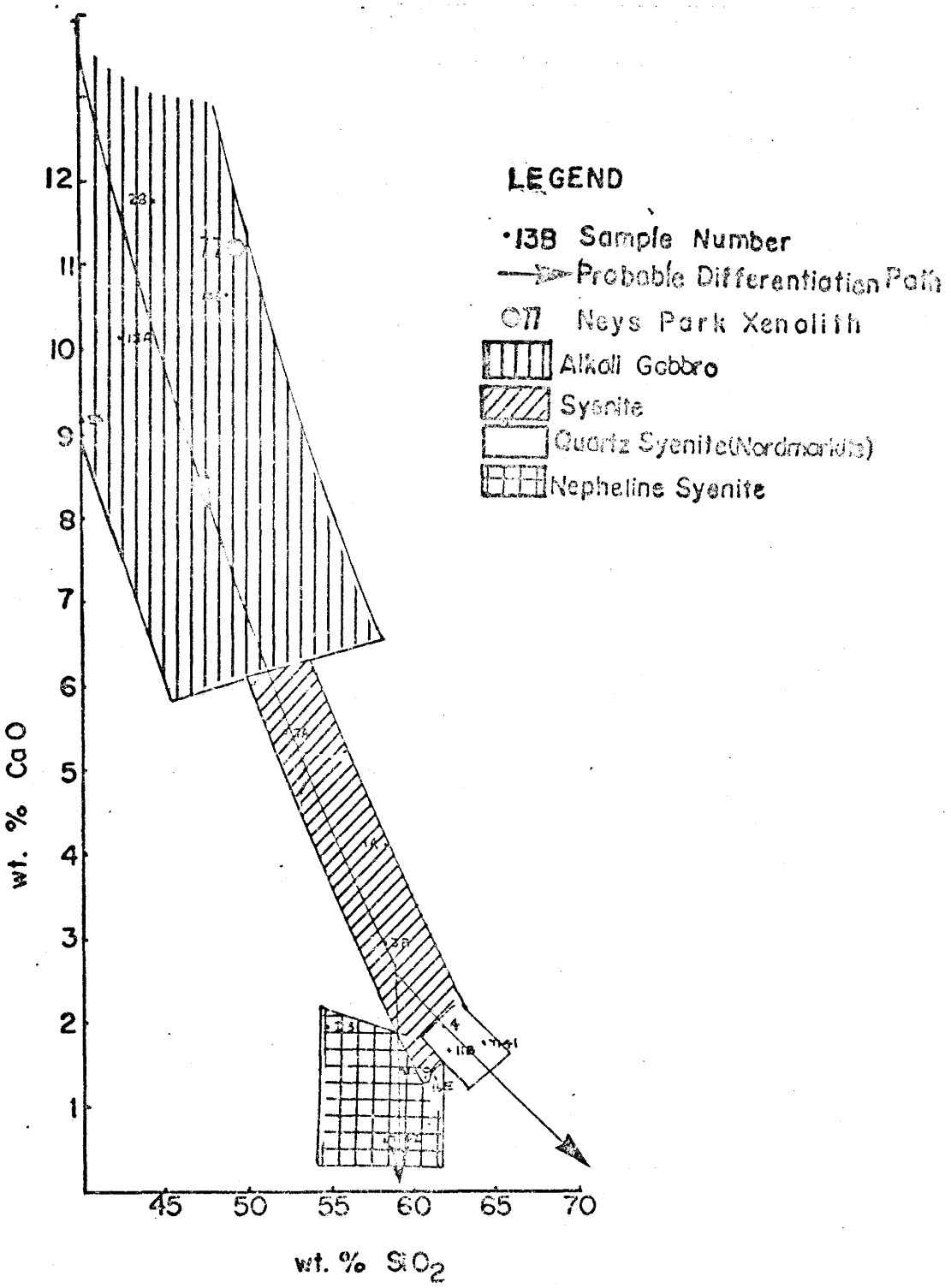

FIG. 12 Weight Percent Silica vs. Lime

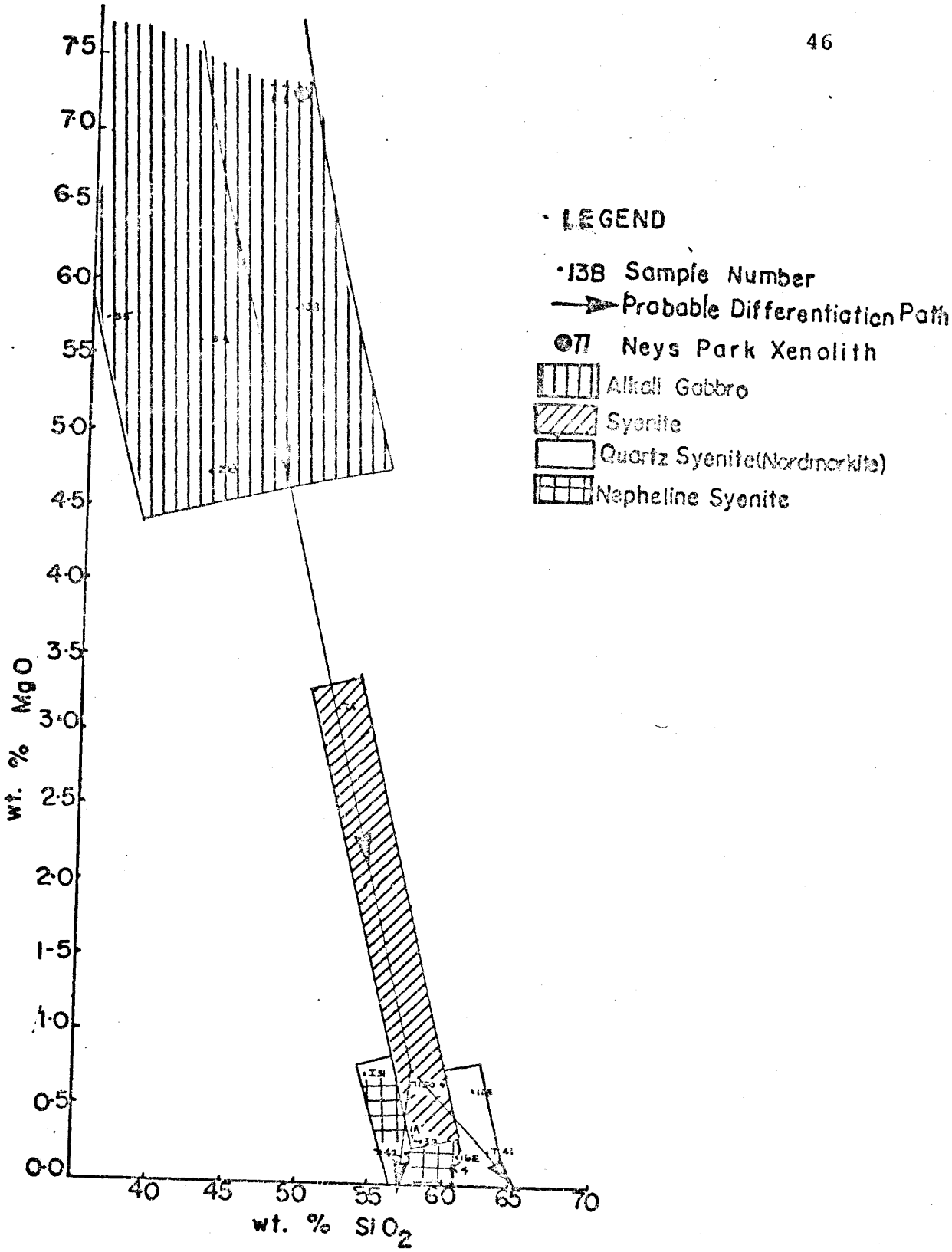

FIG. 13 Weight Percent Silica vs. Magnesium Oxide

phases occupy a region reflecting their low magnesia contents. Separation of magnesia-rich olivine and augite from the alkali gabbro phase could explain the tremendous difference in MgO.

The weight percent silica against aluminum oxides diagram (see Figure 14) shows a very strong split between the quartz and nepheline syenite fields. The fine-grained gabbro from the Neys Park xenolith lies extremely close to the proposed line of liquid descent. The nepheline syenites appear to follow a trend towards aluminum enrichment, whereas the quartz syenites follow one of depletion. The separation of minerals low in alumina would enrich each residual magma in alumina.

The fine-grained gabbro of the Neys Park xenolith often plots near the proposed line of liquid descent on many of the variation diagrams and close to points representing the layered coarse-grained gabbro. This may suggest a genetic connection between the gabbros recognized as belonging to the intrusion and these rocks, previously interpreted as metavolcanic country rocks.

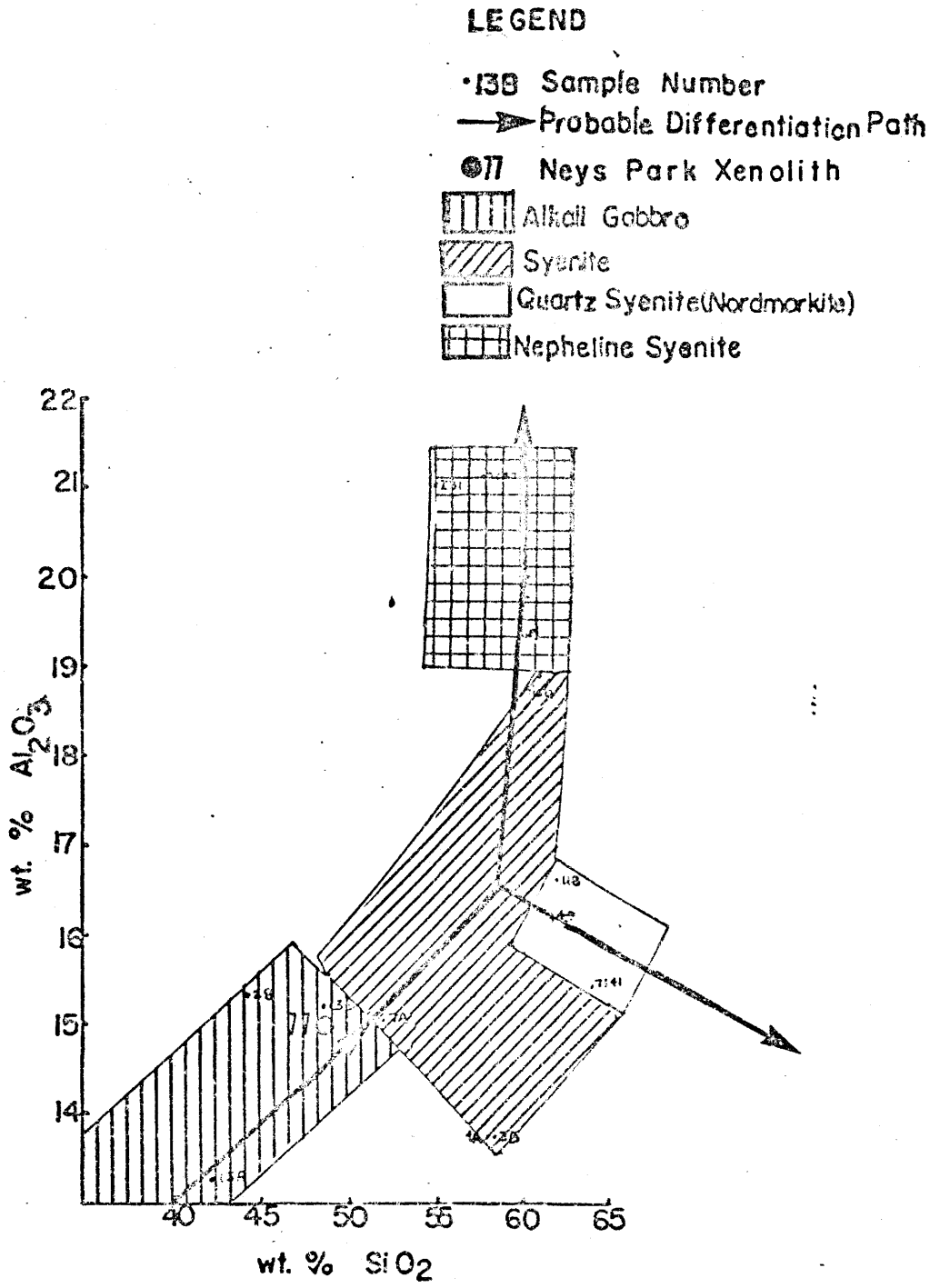

FIG. 14 Weight Percent Silica vs. Aluminum Oxide

CHAPTER 4

AMPHIBOLE CHEMISTRY

Introduction

The amphiboles, kaersutite, barkevekite and arfvedsonite, may represent a solid solution series (Frisch, 1970). Kaersutite and barkevekite are calcium-rich amphiboles, and arfvedsonite is a sodic amphibole. Kaersutite has greater than 2 atoms of Mg in the structural formula (Bose, 1963) and often a high titanium content. Barkevekite has a higher iron content and less than 2 atoms of Mg. The structural formulae of the series is as follows:

Calcium amphiboles

Kaersutite -

$$Ca_2\ Na\ (Mg,\ Fe^{+2}\ Fe^{+3}\ Al,\ Ti)_5\ (Si_{6-7}\ Al_{1-2})\ O_{22}\ (O,\ OH)_2$$

Barkevekite -

$$(Na,\ K)\ Ca_2\ (Fe^{+2},\ Mg)_{3-4}\ Fe^{+3}_{1-2}\ (Si_{5.5-6}\ Al_{2.5-1.5})\ O_{22}\ (OH)_2$$

Alkali amphiboles

Arfvedsonite -

$$(Na_{2-2.5}\ Ca_{0.5-1})\ (Fe^{+2}_{2.5-4}\ Mg_{0.5-1.5})\ Fe^{+3}_{0.5-1.5}\ Si_8O_{22}\ (OH)_2$$

On the basis of the MgO/FeO ratio, kaersutite is expected to form at an earlier stage of crystallization and at a higher temperature of crystallization (Bose, 1963).

Kaersutite-peridotite inclusions have been found in undersaturated host rocks at Grand Canyon, Arizona. The kaersutite originated by precipitation and accumulation of crystals in a deep-seated body of fractionating basaltic magma (Best, 1970). This implies precipitation of kaersutite over a broad range of pressures as high as those in the upper mantle (Best, 1970). Kaersutite-bearing peridotites may constitute significant portions of the upper mantle and crust beneath regions of protracted basaltic volcanism and by partial fusion may generate undersaturated nephelinitic magmas (Best, 1970). The subtraction of a large volume of sub-silicic kaersutite from magmas of intermediate composition, may cause a jump in the silica content of the residual liquids. This may explain the frequently observed silica gap common in many fractionation sequences (Borley, Suddaby and Scott, 1971).

The purpose of the amphibole analysis was to identify the characteristic amphibole of each phase of the Port Coldwell intrusive, and to provide corroborating evidence to support cogenetic relationships interpreted from other sources. Separate analyses of rims and cores of individual amphiboles were to be done using an electron microprobe, in order to see if any zoning

was present and whether this zoning reflected any overall differentiation trends.

The problems inherent in electron microprobe analyses include: surface damage caused by bombardment of the polished thin section by the electron beam; the contamination of the surface of the thin section with polymerized pump oil; the instability of the electron beam, which may result in a filament warpage causing a decrease in the count rate with time; and the difficulty in depositing the same thickness of carbon (used to conduct electrons) on each thin section which results in different count rates (Smith, 1965). Comparison of results obtained through wet chemical techniques to results using the probe indicate a higher value of TiO_2 in the wet chemical method, possibly due to impurities in the cleavage (Rucklidge, Gasparrini, Smith and Knowles, 1971). Alumina analyses by the probe tend to be higher, while soda analyses are not as accurate as wet chemical analysis (Rucklidge et al., 1971). Soda analyses are poor due to high absorption and uncertainty in mass absorption coefficients.

Method of Analysis

Analyses of the amphiboles were done with a Cambridge Instruments Mark 5 (Microscan) electron microprobe. The probe used three crystals: quartz, KAP and mica. The probe has a 75°

take-off angle. The acceleration voltage was 15 kv and the specimen current, measured on pure iron, was 50-60 nanoamps.

The analyses were made on carbon-coated polished thin sections. Crystals to be analysed were preselected and circled on each section. At least ten readings were recorded for each element per sample. Fluorescence, the indirect production of characteristic X-rays by other elements in the matrix, was minimized by analysing only large crystals free of inclusions. In order to minimize the volatilization of light elements, such as sodium, a low (15 kv) beam voltage was used. When analyzing for light elements, the spot diameter was increased to minimize surface damage. A long instrument warm-up time helped to reduce instrument drift.

The standards for analysis consisted of a synthetic pyroxene (Boettcher) for the elements Ca, Mg and Si, synthetic phlogopite for the elements K and Al, pure iron for the element Fe, ilmenite for the element Ti, and jadeite (British Museum) for the element Na. The standards were read at least twice during each run.

Correction factors for the raw probe data, such as those for background, dead time, atomic number and K-alpha fluorescence, were applied through Empadr 7, a computer programme (Rucklidge and Gasparrini, 1969). Data for both the sample and the standard are compared with theoretical X-ray yields from 100% pure elements. As a consequence of this, the concentrations of the elements in

Table 5. Electron microprobe mineral analyses of amphiboles

	7A r	7A c	7A-2	5 r	5-2r	5-2c	5-3	16A r	16A c	27B-1	27B-2	27B-3	27B-4
SiO_2	42.16	42.47	40.25	40.89	40.91	41.11	40.84	39.92	40.38	37.98	39.20	38.96	39.21
Al_2O_3	10.01	9.87	11.60	11.69	11.89	11.94	14.10	14.67	14.29	16.59	12.17	12.49	12.18
Fe_2O_3	1.41	1.29	1.50	1.05	1.12	1.03	1.09	0.98	0.98	1.45	1.45	1.50	1.51
TiO_2	2.43	2.62	1.91	1.67	2.01	1.90	1.67	1.46	1.39	2.58	0.94	1.14	0.75
MgO	8.18	9.32	6.96	8.37	8.65	9.43	8.84	10.76	10.79	7.35	7.93	7.81	7.82
FeO	18.75	17.15	19.97	13.88	14.84	13.73	14.55	13.06	12.99	19.30	19.30	19.96	20.13
CaO	10.98	10.82	10.63	11.13	11.19	11.52	11.46	12.02	11.91	11.18	11.19	11.48	10.97
Na_2O	2.15	2.14	2.15	2.80	2.55	2.60	2.60	2.62	2.46	2.08	2.53	2.26	2.16
K_2O	1.60	1.54	1.74	1.72	1.66	1.61	1.84	1.00	1.05	1.70	1.78	1.62	1.85

Samples 7A to 5-3 - from syenites

Samples 16A to 27B-4 - from lamprophyre dykes

r - rim analysis

c - core analysis

Table 5/continued

	72-1r	72-1c	72-2r	72-2c	131-1r	131-1c	131-2r	131-2c	16E c	16E r	7141r	7141-2
SiO_2	36.94	36.79	37.10	38.94	38.89	38.78	39.27	39.33	35.19	39.22	46.82	44.02
Al_2O_3	9.76	9.85	11.09	11.18	10.90	10.90	11.29	11.10	11.50	10.09	3.87	5.25
Fe_2O_3	2.16	2.19	2.18	1.98	1.56	1.54	1.49	1.58	1.53	1.93	2.27	2.32
TiO_2	2.37	1.30	2.50	2.63	2.12	2.24	2.29	1.89	2.41	1.83	1.58	0.23
MgO	2.66	2.02	2.08	3.23	5.95	6.35	6.90	6.48	3.85	3.10	2.06	1.69
FeO	28.75	29.15	28.92	26.26	20.68	20.51	19.79	20.99	20.26	25.64	30.14	30.80
CaO	9.19	9.54	9.53	10.31	11.14	11.22	11.06	11.23	17.62	10.67	8.19	8.13
Na_2O	2.40	2.33	2.34	2.38	2.11	2.11	2.07	2.09	2.82	2.91	1.92	0.35
K_2O	1.68	1.71	1.80	1.68	1.79	1.67	1.65	1.71	0.76	1.66	1.01	1.20

Samples 72-1 to 131-2 - from nepheline syenites

Samples 16E to 7141-2 - from quartz syenite

r - rim analysis

c - core analysis

Table 5/continued

	65	26A r	26A c	26A-2r	26A-2c	26A-3r
SiO_2	53.69	49.62	50.12	49.37	48.85	49.41
Al_2O_3	0.60	0.97	0.78	0.97	0.98	0.63
Fe_2O_3	2.09	2.39	2.36	2.39	2.36	2.37
TiO_2	1.17	0.70	0.81	0.79	0.72	0.86
MgO	0.00	0.00	0.00	0.00	0.00	0.00
FeO	27.81	31.70	31.30	31.59	31.30	31.50
CaO	0.15	2.21	1.14	2.21	2.31	1.18
Na_2O	9.67	4.74	5.20	4.78	4.87	5.00
K_2O	0.01	1.42	1.58	1.34	1.26	1.55

Samples 65 to 26A-3 - from granite

r - rim analysis

c - core analysis

the standards do not have to be close to those in the amphibole being analysed.

The mineral formulae of the amphiboles were calculated from the oxide chemical analyses (obtained from the probe) on the basis of 23 oxygens (Jackson, Stevens and Bowen, 1967). The total iron from the probe analysis was recalculated to Fe_2O_3 and FeO by determining the ratio of the two species in an amphibole from the laurvikite phase. The assumption was made that the ratio, obtained by wet chemical analysis, was constant for all the amphiboles of the intrusion.

Elemental Trends in Port Coldwell Amphiboles

The following elemental trends in Port Coldwell amphiboles were observed:

1. Increasing values of Niggli mg, which corresponds to increasing basicity of the amphibole, may reflect the differentiation sequence of the parent rock from which the amphibole was derived. In the case of the Port Coldwell amphiboles, there is a decrease in the value of the Niggli mg from syenite and lamprophyre to nepheline syenite to nordmarkite to granite. This trend in the amphiboles favourably reproduces the differentiation trend indicated in the whole rock chemical analyses data interpretation.

2. Na shows a relatively constant value through the phases exhibiting higher Niggli mg values, but increases sharply in the granite, which is the phase with lowest Niggli mg. A similar behaviour is encountered with Si.

3. Ca shows a constant decrease with decreasing Niggli mg. The pattern is higher Ca values in the syenites and lamprophyres, with lowering values in the nepheline syenites, nordmarkites and granites (see Figure 15). Mg and Al have a similar behaviour.

4. Fe has the reverse relationship to Ca, Mg and Al, showing a constant increase with decreasing Niggli mg. This may indicate an enrichment of Fe with differentiation.

5. Ti and K appear to exhibit no response to changes of phase.

6. The lamprophyre dykes which cut all other phases of the Port Coldwell intrusion, appear to exhibit similar elemental values and trends in their amphiboles. The Niggli mg values are within the syenite range. This trend may indicate a cogenetic relationship with the other phases of the Port Coldwell alkali intrusive.

7. No pattern of increase or decrease of elements from rim to core in the amphiboles was detectable.

The plot of alkali, iron and magnesia (AFM) components of the Port Coldwell amphiboles (see Figure 16) exhibits a series of overlapping fields. These fields represent the amphiboles from the various phases. The trend begins in the lamprophyre and syenites then leads to the nepheline syenites then the nordmarkites (quartz syenites), and finally to a separate, distinct field occupied by the arfvedsonitic amphiboles of the granitic phase. This trend syenite-nepheline-quartz syenite-granite is similar to the trends suggested by plots of whole rock chemical analysis data (see Figures 8-15). The kaersutitic amphiboles from the lamprophyre dykes overlap the field of the amphiboles from the syenites at the beginning of the differentiation trend. This suggests that the lamprophyre dykes may have been derived from a primitive magma late in time, rather than from later phases such as the syenitic phase. Stratigraphically the lamprophyre dykes cut all the other phases of the Port Coldwell intrusive except the granites.

Variation in Amphibole Type with Phases of the Port Coldwell Intrusive

The amphibole which occurs in the laurvikitic phase of the Port Coldwell alkali intrusive is a calcium-rich amphibole, kaersutite (see Table 6). These kaersutites have a relatively high iron content (up to 2 atoms Fe) and a low Ti content (approximately

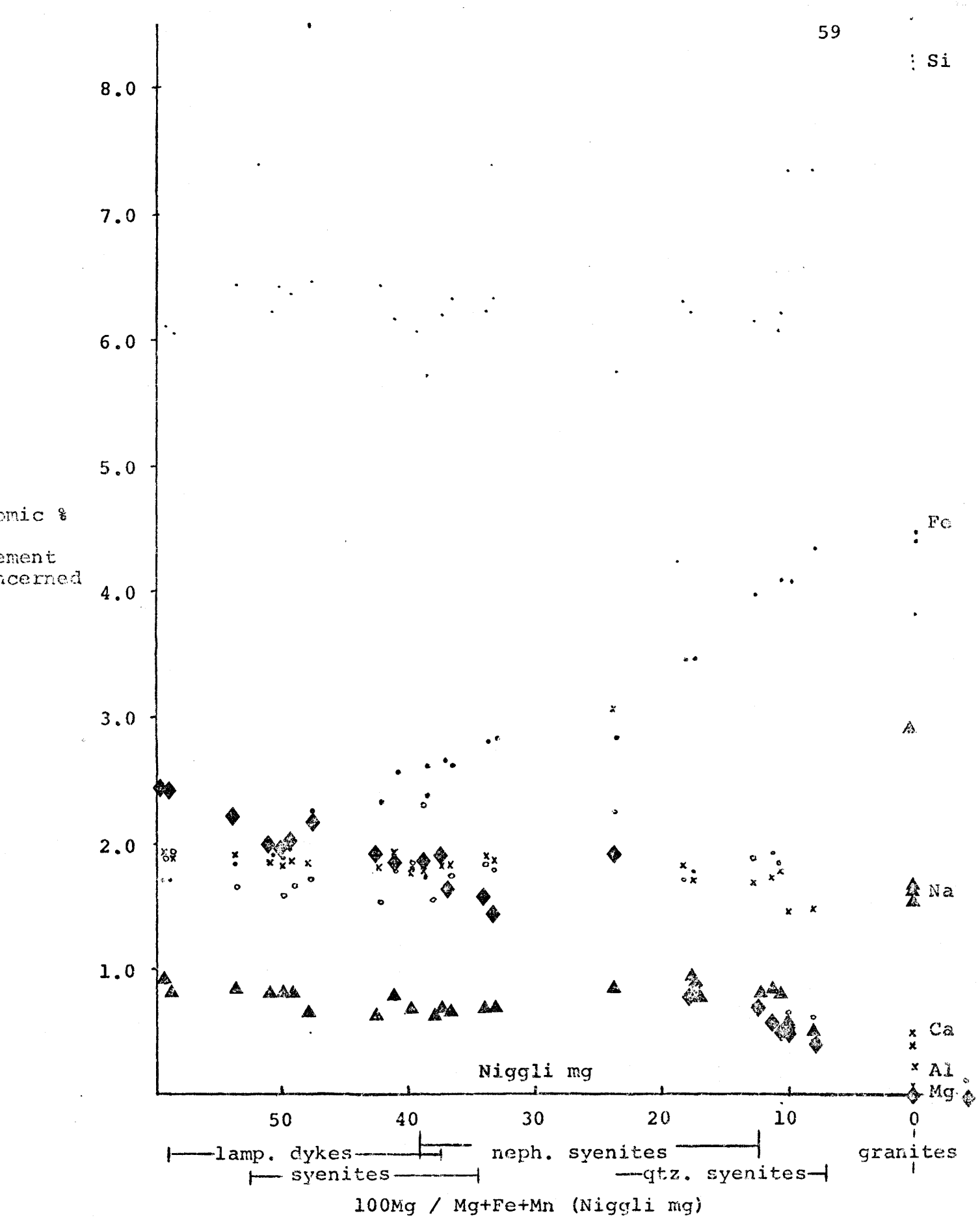

Figure 15. Port Coldwell Amphiboles: plot of atomic % vs. Niggli mg (rock types also indicated)

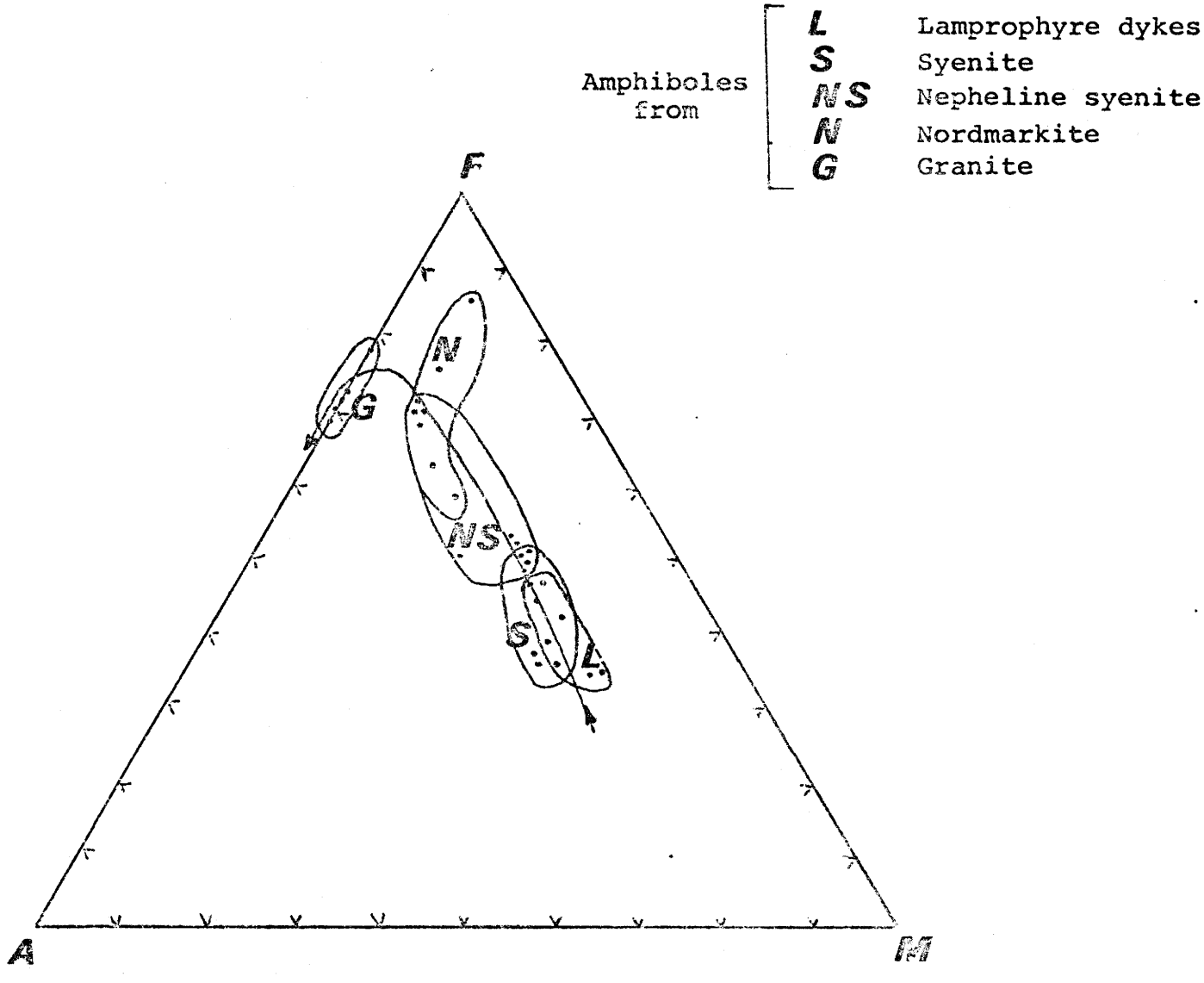

Figure 16. AFM plot (in atomic %) for Port Coldwell amphiboles showing possible differentiation trend

2.5 atoms). These amphiboles appear to be differentiating towards an amphibole of barkevekitic composition, which is another Ca-rich amphibole differing from the kaersutites by a dominant iron content relative to magnesium (less than 2 atoms). Some amphiboles from the laurvikite possess a composition intermediate between these two solid solution series members (see Table 6).

The amphibole within the nepheline syenite phase is a barkevekite with up to 4 atoms of Fe^{+2}. Values of Ti are similar to those of the kaersutites of the syenites, although Mg values are much lower. The quartz syenite phase (nordmarkite) also has a barkevekitic amphibole similar to those in the nepheline syenites, although there is a higher sodium content in the former (see Table 6).

The amphibole contained in the granitic phase of the Port Coldwell intrusive is an arfvedsonite (see Table 6). These arfvedsonites contain up to 2.97 sodium atoms, and unlike the amphiboles of the other phases of the Port Coldwell intrusive, has no Mg.

The trend from a kaersutitic amphibole contained in a syenitic phase to a barkevekitic amphibole in a nepheline syenite phase to an arfvedsonitic amphibole in a granitic phase is similar to trends found in other alkali intrusions, such as those of the Sakhalin Islands (Yagi, 1953) and Monteregian intrusions (Frisch, 1970).

Table 6. Amphibole structural formulae

Amphiboles from laurvikite phase:

Amphibole 7A (rim)

(Na 0.44 K 0.31)	(Ca 1.80 Na 0.20)	(Ti 0.28 Fe^{+3} 0.16 Fe^{+2} 2.40 Mg 1.87 Al 0.27)	(Al 1.54 Si 6.46)
0.75	2.00	4.98	8.00

Amphibole 7A (core)

(Na 0.40 K 0.30)	(Ca 1.77 Na 0.23)	(Ti 0.30 Fe^{+2} 2.19 Fe^{+3} 0.15 Mg 2.12 Al 0.26)	(Al 1.52 Si 6.48)
0.70	2.00	5.02	8.00

Amphibole 7A (interstitial crystal)

(Na 0.43 K 0.35)	(Ca 1.78 Na 0.22)	(Ti 0.22 Fe^{+2} 2.61 Fe^{+3} 0.17 Mg 1.62 Al 0.42)	(Al 1.71 Si 6.29)
0.78	2.00	5.04	8.00

Amphibole 5 (rim)

(Na 0.63 K 0.33)	(Ca 1.86 Na 0.14)	(Ti 0.24 Fe^{+2} 1.93 Fe^{+3} 0.13 Mg 2.00 Al 0.54)	(Al 1.64 Si 6.36)
0.96	2.00	4.84	8.00

Amphibole 5 (core)

(Na 0.69 K 0.32)	(Ca 1.91 Na 0.09)	(Ti 0.22 Fe^{+2} 1.76 Fe^{+3} 0.12 Mg 2.17 Al 0.53)	(Al 1.64 Si 6.36)
1.01	2.00	4.80	8.00

Amphibole 5 (crystal number 2)

(Na 0.62 K 0.35)	(Ca 1.86 Na 0.14)	(Ti 0.19 Fe^{+2} 1.85 Fe^{+3} 0.12 Mg 2.00 Al 0.71)	(Al 1.81 Si 6.19)
0.97	2.00	4.87	8.00

Table 6/continued

Amphiboles from the lamprophyre dykes:

Amphibole 16A (rim)

(Na 0.72 K 0.19)	(Ca 1.95 Na 0.05)	(Ti 0.17 Fe^{+2} 1.65 Fe^{+3} 0.11 Mg 2.43 Al 0.65)	(Al 1.89 Si 6.11)
0.91	2.00	5.01	8.00

Amphibole 16A (core)

(Na 0.65 K 0.20)	(Ca 1.93 Na 0.07)	(Ti 0.29 Fe^{+2} 2.43 Fe^{+3} 0.29 Mg 1.65 Al 0.65)	(Al 1.89 Si 6.11)
0.85	2.00	5.00	8.00

Amphibole 27B

(Na 0.41 K 0.33)	(Ca 1.80 Na 0.20)	(Ti 0.29 Fe^{+2} 2.43 Fe^{+3} 0.16 Mg 1.65 Al 0.65)	(Al 2.29 Si 5.71)
0.74	2.00	5.18	8.00

Amphibole 27B (crystal 2)

(Na 0.65 K 0.36)	(Ca 1.88 Na 0.12)	(Ti 0.11 Fe^{+2} 2.53 Fe^{+3} 0.17 Mg 1.86 Al 0.41)	(Al 1.85 Si 6.15)
1.01	2.00	5.08	8.00

Amphibole 27B (crystal 3)

(Na 0.60 K 0.32)	(Ca 1.92 Na 0.08)	(Ti 0.13 Fe^{+2} 2.61 Fe^{+3} 0.18 Mg 1.82 Al 0.38)	(Al 1.92 Si 6.08)
0.92	2.00	5.12	8.00

Amphibole 27B (crystal 4)

(Na 0.51 K 0.37)	(Ca 1.85 Na 0.15)	(Ti 0.09 Fe^{+2} 2.65 Fe^{+3} 0.18 Mg 1.83 Al 0.42)	(Al 1.84 Si 6.16)
0.88	1.88	5.17	8.00

Table 6/continued

Amphiboles from the nepheline syenite phase:

Amphibole 131 (rim)

$(Na\ 0.58\ K\ 0.37)$	$(Ca\ 1.92\ Na\ 0.08)$	$(Ti\ 0.26\ Fe^{+2}2.78\ Fe^{+3}0.18\ Mg\ 1.42\ Al\ 0.30)$	$(Al\ 1.76\ Si\ 6.24)$
0.95	2.00	2.94	8.00

Amphibole 131 (core)

$(Na\ 0.58\ K\ 0.34)$	$(Ca\ 1.92\ Na\ 0.08)$	$(Ti\ 0.27\ Fe^{+2}2.75\ Fe^{+3}0.19\ Mg\ 1.52\ Al\ 0.26)$	$(Al\ 1.79\ Si\ 6.21)$
1.00	2.00	4.99	8.00

Amphibole 131 (crystal 2 - core)

$(Na\ 0.55\ K\ 0.34)$	$(Ca\ 1.91\ Na\ 0.09)$	$(Ti\ 0.23\ Fe^{+2}2.78\ Fe^{+3}0.19\ Mg\ 1.53\ Al\ 0.30)$	$(Al\ 1.88\ Si\ 6.12)$
0.89	2.00	5.03	8.00

Amphibole 131 (crystal 2 - rim)

$(Na\ 0.52\ K\ 0.33)$	$(Ca\ 1.88\ Na\ 0.12)$	$(Ti\ 0.27\ Fe^{+2}2.62\ Fe^{+3}0.18\ Mg\ 1.63\ Al\ 0.32)$	$(Al\ 1.79\ Si\ 6.21)$
0.85	2.00	4.99	8.00

Amphibole 72 (rim)

$(Na\ 0.40\ K\ 0.36)$	$(Ca\ 1.63\ Na\ 0.37)$	$(Ti\ 0.30\ Fe^{+2}3.98\ Fe^{+3}0.27\ Mg\ 0.66\ Al\ 0.02)$	$(Al\ 1.88\ Si\ 6.12)$
0.76	2.00	5.23	8.00

Amphibole 72 (core)

$(Na\ 0.48\ K\ 0.42)$	$(Ca\ 1.72\ Na\ 0.28)$	$(Ti\ 0.16\ Fe^{+2}4.09\ Fe^{+3}0.28\ Mg\ 0.51\ Al\ 0.13)$	$(Al\ 1.12\ Si\ 6.18)$
0.90	2.00	5.17	8.00

Table 6/continued

Amphibole 72 (crystal 2 - rim)

$(Na\ 0.41\ K\ 0.37)_{0.78}$ $(Ca\ 1.67\ Na\ 0.33)_{2.00}$ $(Ti\ 0.31\ Fe^{+2}3.95\ Fe^{+3}0.27\ Mg\ 0.51\ Al\ 0.19)_{5.23}$ $(Al\ 1.95\ Si\ 6.05)_{8.00}$

Amphibole 72 (crystal 2 - core)

$(Na\ 0.48\ K\ 0.34)_{0.82}$ $(Ca\ 1.75\ Na\ 0.25)_{2.00}$ $(Ti\ 0.31\ Fe^{+2}3.48\ Fe^{+3}0.24\ Mg\ 0.76\ Al\ 0.26)_{5.05}$ $(Al\ 3.82\ Si\ 6.18)_{8.00}$

Amphiboles from the quartz syenite (nordmarkite) phase:

Amphibole 7141

$(Na\ 0.11\ K\ 0.25)_{0.36}$ $(Ca\ 1.45\ Mg\ 0.42)_{1.87}$ $(Ti\ 0.03\ Fe^{+2}4.28\ Fe^{+3}0.29\ Al\ 0.35)_{4.95}$ $(Al\ 0.69\ Si\ 7.31)_{8.00}$

Amphibole 7171 (crystal 2)

$(Na\ 0.04\ K\ 0.21)_{0.25}$ $(Ca\ 1.43\ Na\ 0.57)_{2.00}$ $(Ti\ 0.19\ Fe^{+2}4.11\ Fe^{+3}0.28\ Mg\ 0.50\ Al\ 0.06)_{5.14}$ $(Al\ 0.69\ Si\ 7.31)_{8.00}$

Amphibole 16E

$(Na\ 0.75\ K\ 0.34)_{1.09}$ $(Ca\ 1.84\ Na\ 0.16)_{2.00}$ $(Ti\ 0.22\ Fe^{+2}3.46\ Fe^{+3}0.23\ Mg\ 0.75\ Al\ 0.24)_{4.90}$ $(Al\ 1.67\ Si\ 6.33)_{8.00}$

Amphiboles from the granitic phase:

Amphibole 26A (rim)

$(Na\ 1.52\ K\ 0.30\ Ca\ 0.39)_{2.21}$ $(Ti\ 0.09\ Fe^{+2}4.38\ Fe^{+3}0.30\ Al\ 0.19)_{4.96}$ $(Si\ 8.21)$

Table 6/continued

Amphibole 26A (core)

$$\underline{(Na\ 1.67\ K\ 0.33\ Ca\ 0.20)}_{2.20}\ \underline{(Ti\ 0.10\ Fe^{+2}4.33\ Fe^{+3}0.29\ Al\ 0.15)}_{4.87}\ (Si\ 8.30)$$

Amphibole 26A (crystal 2 - rim)

$$\underline{(Na\ 1.54\ K\ 0.28\ Ca\ 0.39)}_{2.21}\ \underline{(Ti\ 0.10\ Fe^{+2}4.38\ Fe^{+3}0.30\ Al\ 0.19)}_{4.97}\ (Si\ 8.19)$$

Amphibole 26A (crystal 2 - core)

$$\underline{(Na\ 1.58\ K\ 0.27\ Ca\ 0.41)}_{2.26}\ \underline{(Ti\ 0.09\ Fe^{+2}4.38\ Fe^{+3}0.30\ Al\ 0.19)}_{4.96}\ (Si\ 8.18)$$

Amphibole 26A (crystal 3)

$$\underline{(Na\ 1.62\ K\ 0.33\ Ca\ 0.21)}_{2.16}\ \underline{(Ti\ 0.11\ Fe^{+2}4.41\ Fe^{+3}0.30\ Al\ 0.12)}_{4.94}\ (Si\ 8.27)$$

Amphibole 65

$$\underline{(Na\ 2.97\ Ca\ 0.03)}_{3.00}\ \underline{(Ti\ 0.14\ Fe^{+2}3.68\ Fe^{+3}0.25\ Al\ 0.11)}_{4.18}\ (Si\ 8.50)$$

CHAPTER 5

CONCLUSIONS

The Port Coldwell intrusion is a miaskitic intrusion located near the reported triple junction of three gravity-magnetic highs. The complex probably is the result of penecontemporaneous intrusion of alkali gabbro and its differentiation products. The classical differentiation sequence was from a parental alkali gabbro, which by the separation of ilmenomagnetite and Fe-Mg pyroxene, gave rise to a syenitic magma that differentiated to produce the nepheline syenites by a trend towards undersaturation. The same syenitic magma may have assimilated some silica-rich country rocks, starting the magma on an opposing oversaturation trend to produce the quartz syenites and granites of the intrusion.

The lamprophyre dykes, stratigraphically the youngest, may have been derived from a primitive magma late in the differentiation sequence. The field occurrence of carbonate ocelli in the lamprophyre dykes of the Port Coldwell intrusion can best be explained using a liquid immiscibility model.

The ophitic, fine-grained gabbros located north of Neys Provincial Park, which were previously interpreted as a meta-volcanic roof pendant, are a phase of the Port Coldwell intrusion related to the coarser-grained alkali gabbro. Its slightly lower alkalinity may be due to a higher degree of partial melting

as a result of differentiation higher in the crust. Lower iron and titanium contents suggest that if these rocks were differentiated from the same parental magma as the coarser-grained gabbros, they may have formed as a later phase after the separation of the ilmenomagnetite segregations.

The large volume of syenitic rocks relative to the parental gabbros may be due to the previous mapping of substantial volumes of fine-grained gabbros as metavolcanic roof pendants. On the other hand, fractionation of a primary alkali gabbro may have given rise to a lower density, more volatile-rich syenitic magma which rose to higher crustal levels. At a deeper erosional level, more gabbro would be expected to appear.

Magma conditions in the alkali gabbro were such that there was probably locally high oxygen fugacity in order to have precipitated the ilmenomagnetite segregations. The presence of fluorite in the syenites suggests a high fluorine fugacity, and the presence of calcite in the nepheline syenites and lamprophyre dykes indicates a high CO_2 fugacity. A rise in water fugacity within the granitic phase may have caused the unmixing of the perthitic feldspars that are common to all the other phases of the Port Coldwell intrusion. The separation of the perthites found even in the quartz syenites, into a two feldspar system, could not have occurred at water pressures much less than 4000 kg/cm^2, unless much subsolidus rearrangement took place for which there is no evidence.

The Port Coldwell amphiboles show a definite increase in iron with increasing Niggli mg (Mg/Mg+Fe). The increase in values of Niggli mg of the amphiboles from the granitic phase to quartz syenites to nepheline syenites to syenites and lamprophyre dykes, correlates with the decreasing basicity of the host rocks. With decreasing values of Niggli mg there is a decrease in Mg, Al and Ca in the amphiboles. Na and Si values are relatively constant except for a sharp increase within the amphiboles of the granitic phase.

The amphibole within the syenitic phase is a kaersutite which sometimes possesses characteristics intermediate with barkevekite. The amphiboles in the nepheline syenite and quartz syenite phases are barkevekites, while those in the granites are arfvedsonites. These amphiboles, which may represent a solid solution series, suggest a differentiation sequence of cogenetic host rocks.

BIBLIOGRAPHY

AOKI, K., 1963, Kaersutites and oxykaersutites from Japan. Jour. Petrol., 4, pt. 2, 198-210.

BEST, M.G., 1970, Kaersutite-peridotite inclusions and kindred megacrysts in basanitic lavas, Grand Canyon, Arizona. Contr. Mineral. and Petrol., 27, 25-44.

BILL, H., SIERRO, J. and LACROIX, M., 1967, Origin of coloration in some fluorites. Amer. Mineral., 52, no. 7, 1003-8.

BORLEY, G.D., SUDDABY, P. and SCOTT, P., 1971, Some xenoliths from the alkalic rocks of Teneriffe, Canary Islands. Contr. Mineral. and Petrol., 28.

BOSE, M.K., 1963, Calciferous brown amphibole in alkalic gabbro of Koraput, Orissa, India. Amer. Mineral., 48, 12, 1405-9.

CARSTENS, H., 1958, The origin of feldspar inclusions in the lamprophyres of Kistansand, South Norway. Norsk Geol. Tidsskr., 38, 245-52.

CONGRIERE, F., 1971, The amphibole lherzolite from Carisson (Ariege, France). Contr. Mineral. and Petrol., 30, 296-313.

CURRIE, K.L., 1970, An hypothesis on the origin of alkaline rocks suggested by the tectonic setting of the Montergian Hills. Can. Mineral., 10, 3, 411-20.

DALVI, A., 1969, The electron probe microanalyzer. Dept. Metallurgy and Materials Science, McMaster Univ., Hamilton, Ontario, Canada.

EDGAR, A.D., 1965, The mineralogical composition of some nepheline alteration products. Amer. Mineral., 50, 8, 978-89.

ERNST, W.G., 1968, Amphiboles. Springer-Verlag N.Y. Inc.

FERGUSON, J. and CURRIE, K.L., 1971, Evidence of liquid immiscibility in alkaline ultrabasic dikes at Callander Bay, Ontario. Jour. Petrol., 12, 3, 561-85.

FERGUSON, J. and CURRIE, K.L., 1972, Silicate immiscibility in the ancient basalt of the Barberton Mountain land, Transvaal. Nature Phys. Sci., 235

FRISCH, T., 1970, Chemical variations among the amphiboles of Shefford Mountain, a Monteregian intrusion in Southern Quebec. Can. Mineral., 10, 3, 553-70.

GOLD, D.P., 1967, The alkaline ultramafic rocks in the Montreal area, Quebec. In Ultrabasic and Related Rocks (ed. P.J. Wyllie), 288-97.

GREEN, T.H. and RINGWOOD, A.E., 1968, Genesis of the calcalkaline igneous rock suite. Contr. Mineral. and Petrol., 18, 105-74.

GRONLIE, W. and GISLE, P., 1971, Gravity studies of the laurvikite massif, S.W. of Lake Gjerdingen, Nordmarka. Norsk. Geol. Tiddskr., 51, 3, 317-21.

HAUGHTON, D.R., 1967, A Mineralogical Study of Scapolite. Unpub. M.Sc. Thesis, McMaster Univ., Hamilton, Ontario, Canada.

HOWNSLOW, A.W. and MOORE, J.M. Jr., 1966, Preparation and analysis of silicate rocks and minerals. Geol. Paper 66-1, Dept. Geology, Carleton Univ., Ottawa, Canada.

HOWIE, R.A. and SMITH, J.W., 1966, X-ray emission microanalysis of rock-forming minerals, V. Orthopyroxenes. Jour. Geol., 74, no. 4, 443-77.

JACKSON, E.D., STEVENS, R.E. and BOWEN, R.W., 1967, A computer-based procedure for deriving mineral formulas from mineral analyses. U.S.G.S. Prof. Paper 575-C, C23-C31.

KENSON, S. and PRICE, R.C., 1972, The major and trace element chemistry of kaersutite and its bearing on the petrogenesis of alkaline rocks. Contr. Mineral. and Petrol., 35, 119-24.

LE MAITRE, R.W., 1969, Kaersutite-bearing plutonic xenoliths from Tristan da Cunha, South Atlantic. Mineral. Mag., 37, 286, 185-97.

LONG, J.V.P., 1967, Electron probe microanalysis. In Physical Methods of Determinative Mineralogy (ed. J. Zussman), Academic Press, Inc., N.Y.

LUM, H.K., 1973, Petrology of the Eastern Gabbro and Associated Sulfide Mineralization of the Goldwell Alkali Complex, Ontario. Unpub. B.Sc. Thesis, Dept. Geology, Carleton University, Ottawa, Canada.

MATHIAS, M., SEBERT, J.C. and RICKWOOD, P.C., 1970, Some aspects of the mineralogy and petrology of ultramafic xenoliths in kimberlite. Contr. Mineral. and Petrol., 26, 2 , 75-123.

PAPIKE, J.J. and STEPHENSON, N.C., 1966, The crystal structure of mizzonite, a calcium and carbonate rich scapolite. Amer. Mineral., 51, 7

PIOTOWSKI, J. and EDGAR, A.D., 1970, Melting relations of undersaturated alkaline rocks from South Greenland. Meddel.om Gronland, 181, 9, 1-59.

PUSKAS, F.P., 1967, Geology of the Port Coldwell area, district of Thunder Bay. Ont. Dept. Mines, Geol. Branch, Open File Rept. 5014

ROBINSON, P. and JAFFE, H.W., 1969, Chemographic exploration of amphibole assemblages from Central Massachusetts and Southwestern New Hampshire. Mineral. Soc. Amer., Spec. Paper 2, Pyroxenes and Amphiboles: Crystal Chemistry and Phase Petrology

ROSENQUIST, T., 1965, Electron microscope investigations of laurvikite and tonsbergite feldspars. Norsk. Geol. Tiddskr., 45, 69-72.

RUCKLIDGE, J. and GASPARRINI, E.L., 1969, Specifications f a computer program for processing electron microprobe analytical data. Dept. Geology, University of Toronto, Canada.

SAHA, P., 1961, The system NaAlSiO (nepheline)-$NaAlSi_3O_8$ (Albite)-H_2O. Amer. Mineral., 46

SALTER, W.J.M. and JOHNSON, W., 1970, Sources of error in electron microprobe microanalysis. Micron, 2, 2, 157-86.

SMITH, J.V., 1965, X-ray emission microanalysis of rock-forming minerals. I. Experimental techniques. Jour. Geol., 73, no. 6, 830-64.

SMITH, J.V., 1966, X-ray emission microanalysis of rock-forming minerals. VI. Clinopyroxenes near the diopside-hedenbergite join. Jour. Geol., 74, no. 4, 463-77.

SOOD, M.K. and EDGAR, A.D., 1970, Melting relations of undersaturated alkaline rocks. Meddel. om Gronland, 181, no. 12.

SORENSEN, H., 1970, Internal structures and geological setting of the three agpaitic intrusions - Kina and Hovozero of the Kola Peninsula and Ilimavssaq, South Greenland. Can. Mineral., 10, 3, 299-334.

STORMER, J.C. Jr. and CARMICHAEL, I.S.E., 1971, The free energy of sodalite and the behaviour of chloride, fluoride and sulfate in silicate magmas. Amer. Mineral., 56, 292-306.

TUTTLE, O.F. and BOWEN, N.L., 1958, Origin of granite in light of experimental studies. Geol. Soc. Amer., Mem. 74, 153pp.

WATKINSON, D.H., 1971, Experimental studies bearing on the origin of the alkalic rock carbonatite complex and niobium mineralization at Oka, Quebec. Dept. Geology, University of Toronto, Canada.

WATKINSON, D.H., MAINWARING, P.R. and LUM, H.K., 1972, Petrology and copper mineralization of the Coldwell complex, Ontario. Geol. Soc. Amer., Abstr. with Programs, 5, 7

WATKINSON, D.H. and WYLLIE, P.J., 1971, Experimental study of the composition join $NaAlSi_3O_8$-$CaCO_3$-H_2O and the genesis of alkalic rock-carbonatite complexes. Jour. Petrol., 12, 2, 357-78.

WELLMAN, T.R., 1970, The stability of sodalite in a synthetic syenite plus aqueous chloride fluid system. Jour. Petrol., 11, 1, 49-71.

WILKINSON, J.F.G., 1961, Some aspects of the calciferous amphiboles oxyhornblende, kaersutite and barkevekite. Amer. Mineral., 46, 340-54.

WINCHELL, H., 1962, A computer program for handling chemical analyses of amphiboles and other minerals. Amer. Mineral., 47

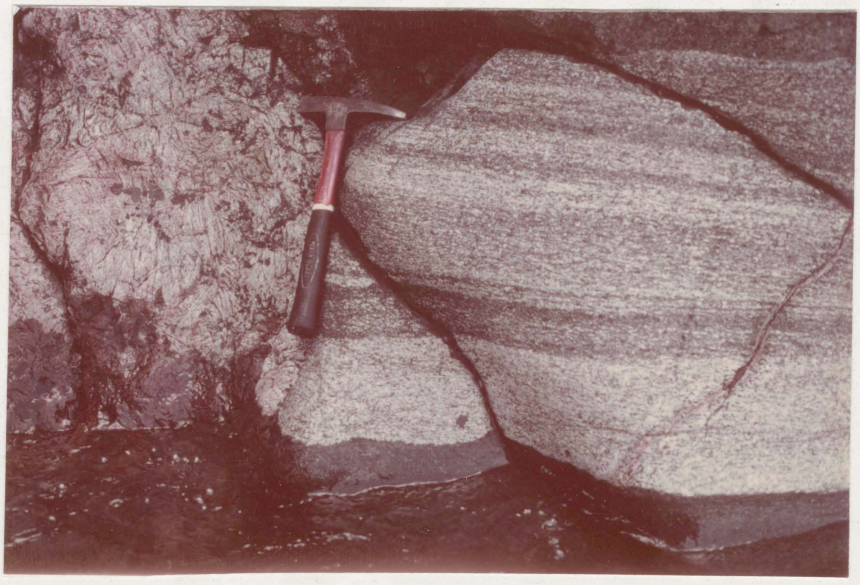

Plate 1 Layered Alkali Gabbro intruded by Syenite Pegmatite Dyke .

Plate 2 Dark Syenite (Laurvikite) showing preferred orientation of Perthite crystals and containing similarly oriented ellipsoidal inclusions of Gabbro.

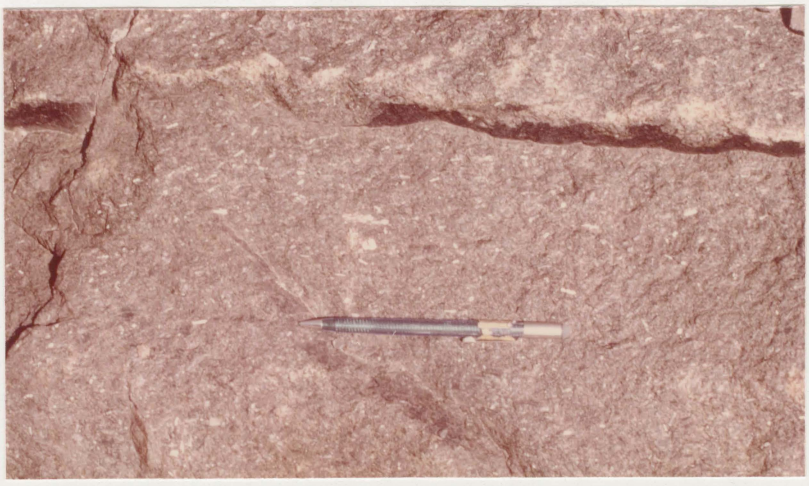

Plate 3 Dark Syenite (Laurvikite) showing linear alignment of Perthite crystals.

Plate 4 Nepheline Syenite Pegmatite intruded by Lamprophyre Dyke and containing xenoliths of Alkali Gabbro.

Plate 5 Zoned Feldspar crystal with Nepheline phenocryst from Nepheline Syenite Pegmatite.

Plate 6 Nepheline Syenite with cyclic irregular layering defined by dark Amphibole-rich laminae.

Plate 7 Melanocratic Nepheline Syenite (Nepheline-poor) containing clots of Leucocratic Nepheline Syenite (Nepheline-rich). The orange-brown mineral is the Nepheline.

Plate 8 Lamprophyre Dyke showing alternating carbonate ocelli-rich layers. Layering is parallel to strike.

Plate 9 Columnar-jointed Lamprophyre Dyke with ellipsoidal carbonate ocelli aligned parallel to strike of the dyke.

Plate 10 Lamprophyre Dyke with Carbonate Segregation at the contact with coarser-grained Alkali Gabbro.

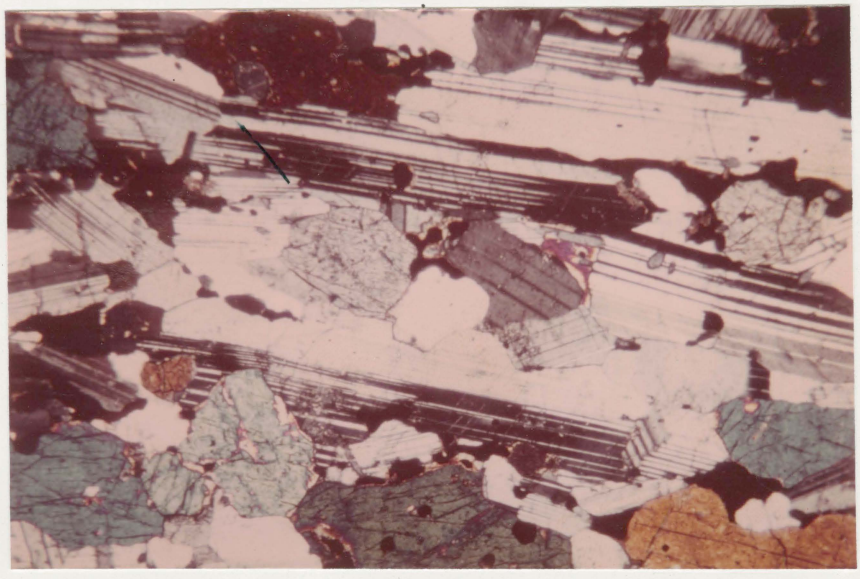

1 mm

Plate 11 Plagioclase-rich layer of the Alkali Gabbro with strong lineation defined by preferred orientation of Labradorite (and Augite). Ilmenomagnetite and Apatite are minor constituents.

(crossed nicols)

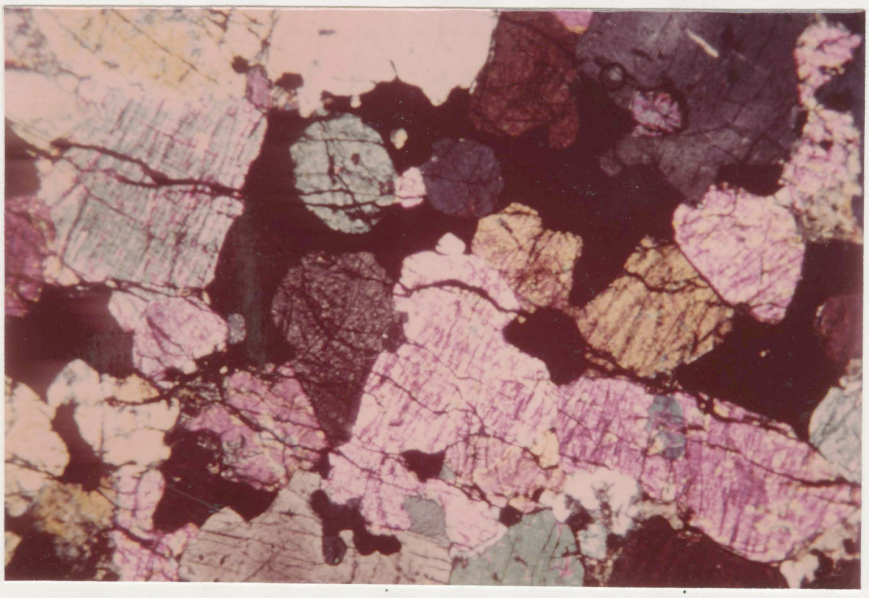

1 mm

Plate 12 Pyroxene and Ilmenomagnetite-rich layer of the Alkali Gabbro. Black areas are the Ilmenomagnetite.

(crossed nicols)

1 mm

Plate 13 Pyroxene-rich layer of the Alkali Gabbro showing hourglass zoning in the Augite crystals. Plagioclase (labradorite) is an interstitial mineral.

(crossed nicols)

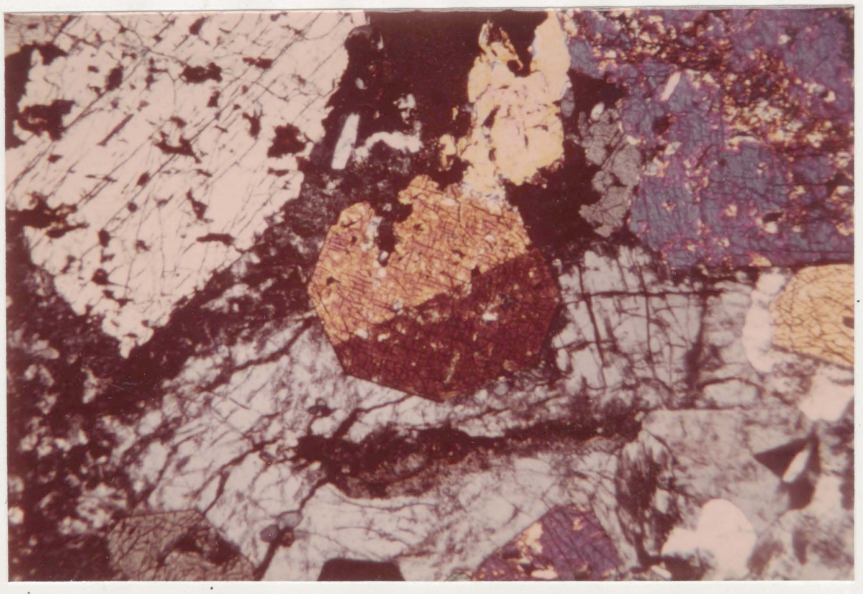

1 mm

Plate 14 Layered Alkali Gabbro with twinned Augite showing typical Pyroxene cleavage. Labradorite and Apatite also present.

(crossed nicols)

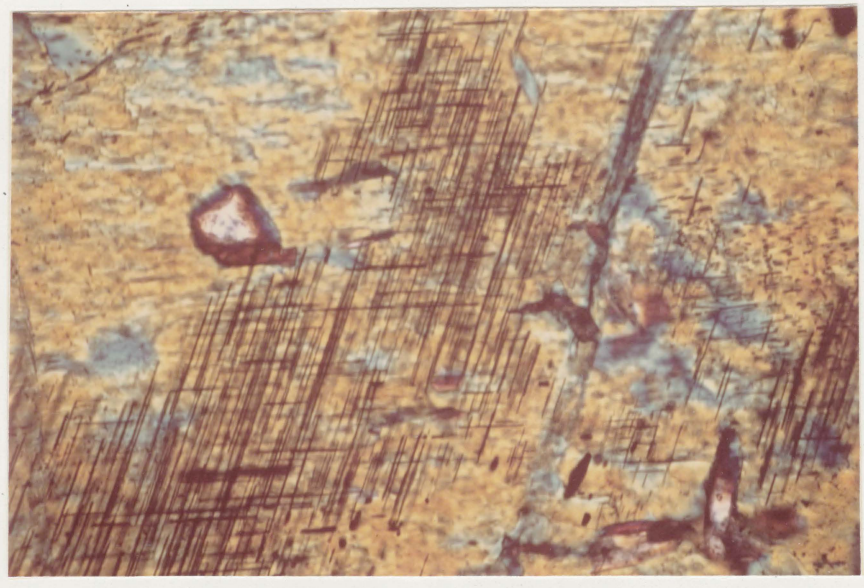

1 mm

Plate 15 Augite from layered Alkali Gabbro showing schiller inclusions of Titaniferous Magnetite. Apatite inclusions are also present.

(crossed nicols)

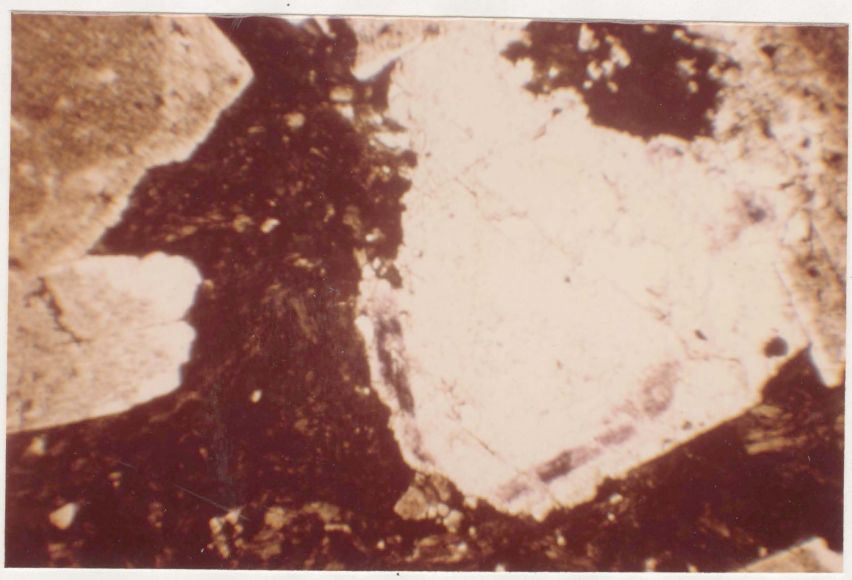

1 mm

Plate 16 Syenite with low relief Flourite which shows purple zoning and perfect octahedral cleavage. Dark anhedral green-brown mineral is an Amphibole. Cloudy altered Alkali Feldspars frame the picture.

(plane light)

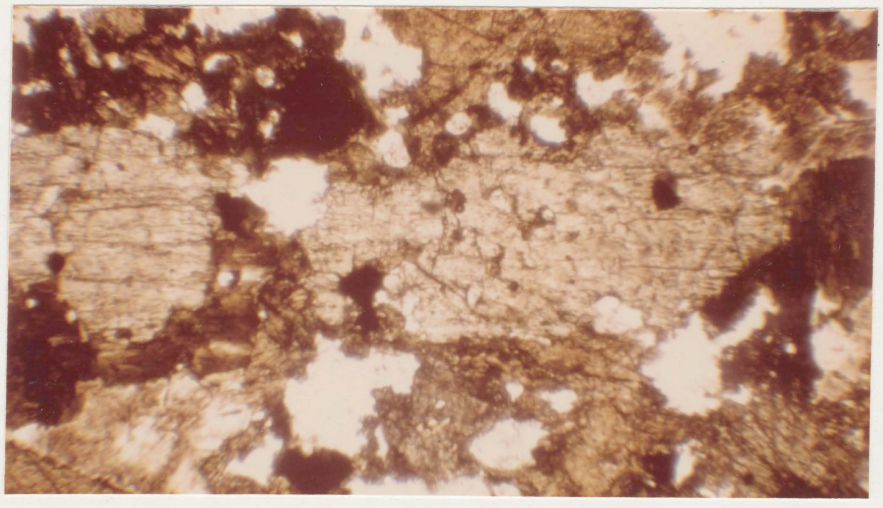

1 mm

Plate 17 Syenite showing pale Pyroxene crystal being marginally altered (uralitized) to a brown Amphibole. Magnetite and Apatite are present as inclusions. Most clear areas are holes.

(plane light)

1 mm

Plate 18 Nepheline Syenite showing weak lineation defined by preferred orientation of partially altered (cloudy) Perthites and almost opaque dark green Amphibole. Anhedral grey mineral on the right border is Hydronephelite (altered Nepheline).

(crossed nicols)

1 mm

Plate 19 Nepheline Syenite showing twinned brown Amphibole surrounded by yellow-green, stained Nepheline. Malachite Green followed by Sodium Cobaltinitrite produced the colouration. Clear areas are holes.

(plane light)

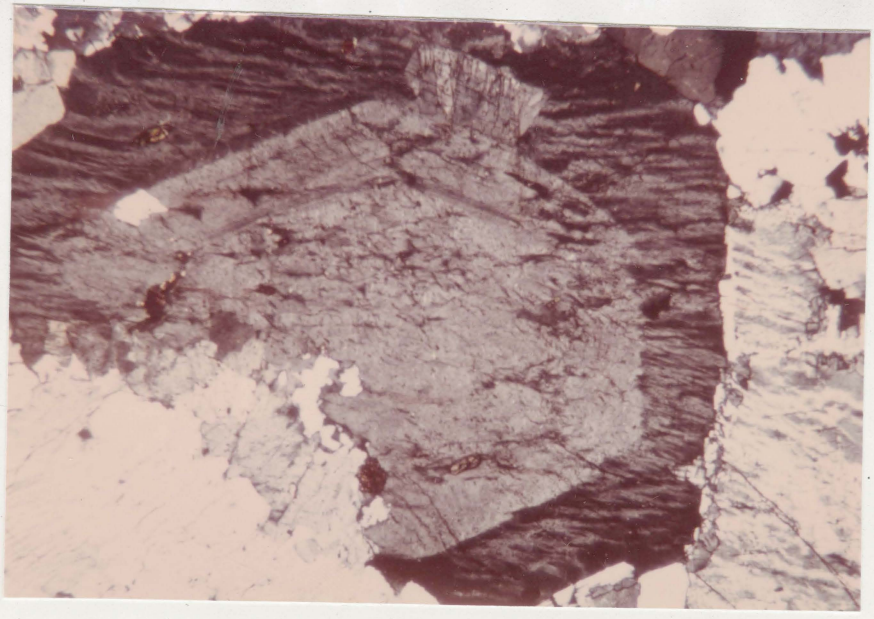

1 mm

Plate 20 Quartz Syenite (Nordmarkite) showing zoned Alkali Feldspar crystal with solvus defined by outer Perthite rim. Perthites surround the crystal. Clear areas and inclusions are Quartz.

(crossed nicols)

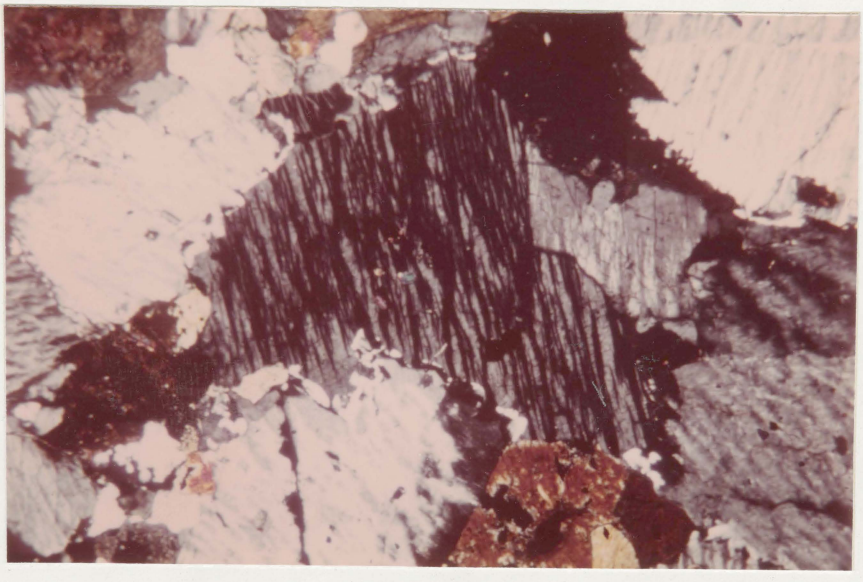

1 mm

Plate 21 Quartz Syenite (Nordmarkite) illustrating typical Perthites. Amphiboles (with medium interference colours) constitute a low modal percent. Clear mineral is Quartz.

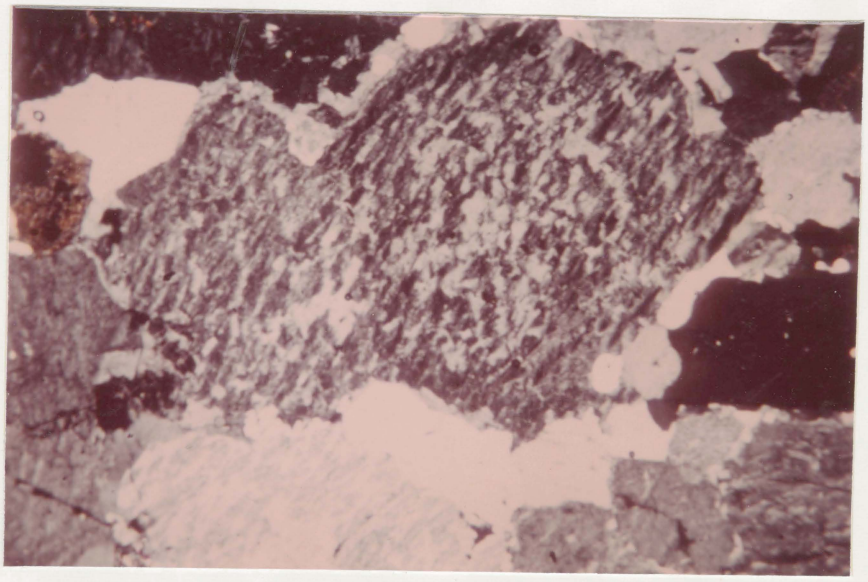

1 mm

Plate 22 Pink Granite showing typical Perthites similar to those of other phases of the intrusion. The clear mineral is Quartz.

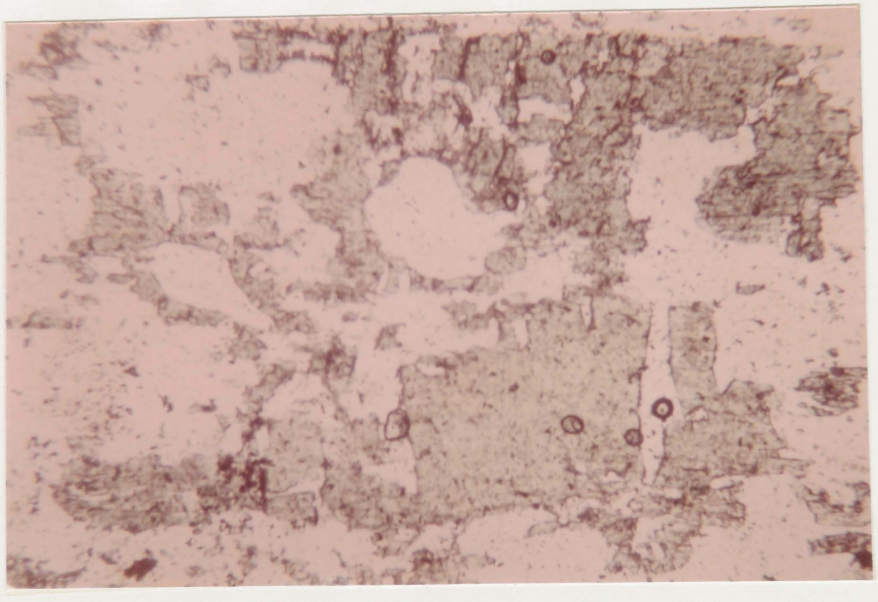

1 mm

Plate 23 Pink Granite showing unstable green Amphibole with abundant Quartz inclusions.

(plane light)

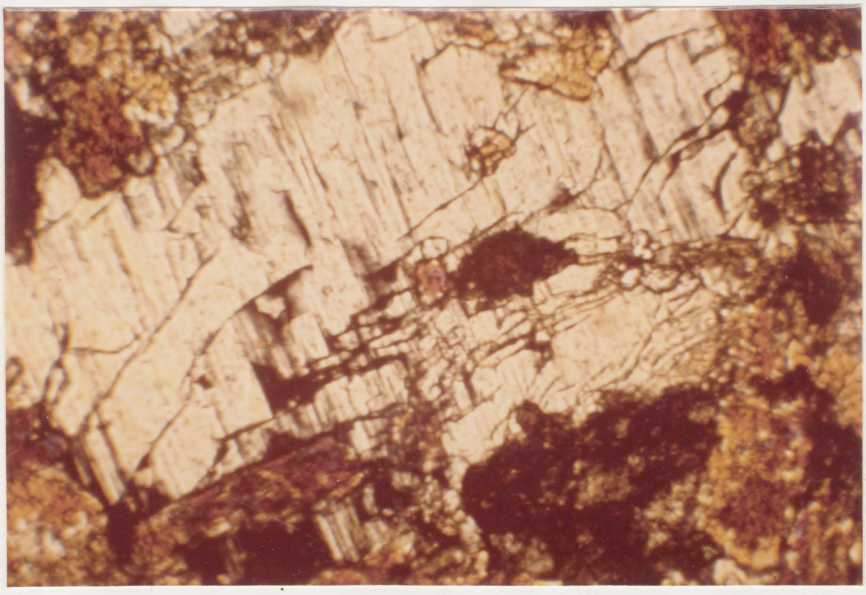

Plate 24 Lamprophyre Dyke [illegible] with Scapolite phenocryst in a matrix of partially altered Amphiboles.

(crossed nicols)

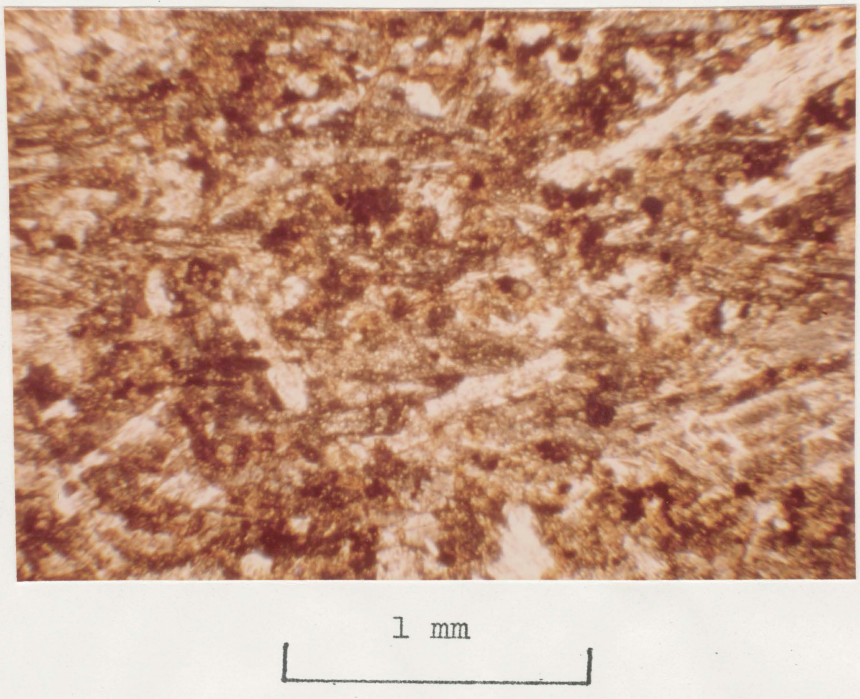

Plate 25 Lamprophyre Dyke (Camptonite) showing Trachytic texture and high degree of deuteric alteration.

1 mm

Plate 26 Camptonite Dyke with Calcite Ocellus surrounded by deuterically altered Labradorite crystals and interstitial Biotite.

Plate 27 Brecciated Alkali Gabbro-Syenite contact showing Pegmatite and fine-grained, thinly layered Alkali Gabbro.

1 mm

Plate 28 Fine-grained Alkali Gabbro near the contact with Syenites. Labrodorite crystals define a weak Lineation. Pyroxene and Ilmenomagnetite are also present.

1 mm

Plate 29 Neys Park Gabbro showing Ophitic texture defined by slightly altered Labradorite and Augite crystals.